Z. Angew. Math. Phys. (2018) 69:18

0044-2275/18/010001-32
published online January 29, 2018
https://doi.org/10.1007/s00033-018-0910-4

Zeitschrift für angewandte Mathematik und Physik ZAMP

Three-dimensional coupled thermoelastodynamic stress and flux induced wave propagation for isotropic half-space with scalar potential functions

Yazdan Hayati and Morteza Eskandari-Ghadi

Abstract. An asymmetric three-dimensional thermoelastodynamic wave propagation with scalar potential functions is presented for an isotropic half-space, in such a way that the wave may be originated from an arbitrary either traction or heat flux applied on a patch at the free surface of the half-space. The displacements, stresses and temperature are presented within the framework of Biot's coupled thermoelasticity formulations. By employing a complete representation for the displacement and temperature fields in terms of two scalar potential functions, the governing equations of coupled thermoelasticity are uncoupled into a sixth- and a second-order partial differential equation in cylindrical coordinate system. By virtue of Fourier expansion and Hankel integral transforms, the angular and radial variables are suppressed respectively, and a 6th- and a 2nd-order ordinary differential equation in terms of depth are received, which are solved readily, from which the displacement, stresses and temperature fields are derived in transformed space by satisfying both the regularity and boundary conditions. By applying the inverse Hankel integral transforms, the displacements and temperature are numerically evaluated to determine the solutions in the real space. The numerical evaluations are done for three specific cases of vertical and horizontal time-harmonic patch traction and a constant heat flux passing through a circular disc on the surface of the half-space. It has been previously proved that the potential functions used in this paper are applicable from elastostatics to thermoelastodynamics. Thus, the analytical solutions presented in this paper are verified by comparing the results of this study with two specific problems reported in the literature, which are an elastodynamic problem and an axisymmetric quasi-static thermoelastic problem. To show the accuracy of numerical results, the solution of this study is also compared with the solution for elastodynamics exists in the literature for surface excitation, where a very good agreement is achieved. The formulations presented in this study may be used as benchmark for other related researches and it may be implemented in the related boundary integral equations.

Mathematics Subject Classification. 35D35.

Keywords. Asymmetric three-dimensional problem, Thermoelastodynamic, Stress wave propagation, Heat flux induced wave propagation, Potential method, Isotropic half-space.

List of symbols

U_r, U_θ, U_z	Displacement components
u_r, u_θ, u_z	Amplitudes of the displacement components
ρ	Density of mass
∇	The gradient operator
∇^2	The Laplacian operator
$\beta = (2\mu + 3\lambda)\,\alpha$	Thermal stress coefficient
α	Thermal expansion coefficient
$\varepsilon = \varepsilon_{rr} + \varepsilon_{\theta\theta} + \varepsilon_{zz}$	Dilatation
c	Specific heat
$T = T_1 - T_0$	Temperature increment
T_1	Absolute temperature
T_0	Reference temperature
k	Thermal conductivity
λ, μ	Lame's constants

π_0	Finite region on the surface
$[P, Q, R(r, \theta, z)]$	Time-harmonic surface traction components in r-, θ- and z-directions respectively
$H(r, \theta, z)$	Time-harmonic heat flux
F, χ	Potential functions
$c_1 = C_{\mathrm{d}}$	Dilatational wave speed
$c_2 = C_{\mathrm{s}}$	Equivoluminal (shear) wave speed
$\lambda_i, (i = 1 - 4)$	Radicals appeared in the general solution
$\xi_{\lambda_i}, (i = 1 - 4)$ and ξ_p	Branch points and pole in the complex ξ plane
ω	Circular frequency of harmonic motion
ω_0	Dimensionless frequency
ξ	Hankel's parameter
E	Young's modulus
υ	Poisson's ratio
J_{m}	Bessel function of first kind and mth order
a	Radius of circular disc
r, θ, z	Radial, angular and vertical coordinates respectively
t	Time variable
$g_i, h_i, l_i, n_i, x_i, y_i, z_i$	Some functions appeared in the general solution
q_0	Constant heat flux distributed on a circular patch of radius a
R and P	Resultant forces
$\lambda_{1\mathrm{e}}, \lambda_{2e} = \bar{\alpha}, \bar{\beta}$	Solutions of the characteristic equation in the case of elastodynamics
$\lambda_{iqs}, (i = 1, 2, 3)$	Solutions of the characteristic equation in the case of quasi-static
$\sigma_{ij}, (i, j = r, \theta, z)$	Stress components

1. Introduction

The theory of coupled thermoelasticity is a need in investigating many phenomena with the applications in the fields of engineering and physical sciences such as structural engineering, earthquake engineering, soil dynamics, aeronautics, astronautics, nuclear reactors, high energy particle accelerator, etc. Thermoelasticity is also a framework, where the stress redistribution in ceramic matrix composites is evaluated on [1,2]. In the field of structural engineering, scientists use their understanding of thermoelasticity to design materials and objects that can withstand fluctuations in temperature without breaking [3]. Understanding the principles of coupled thermoelasticity helps engineers design structures in such a way that they maintain their integrity for a wide range of temperature changes [3]. In the structural engineering, another example is the application of thermoelasticity for remote inspection of fatigue cracks in the steel bridges [4]. Thermoelastic stress analysis (TSA) by infrared thermography has been widely used as an effective full-field experimental stress measurement technique [4]. TSA has been gaining increasing attention as a nondestructive testing and evaluation method for fatigue cracks in steel structures [4]. TSA is extremely beneficial not only for crack detection but also for the on-site measurement of stress distributions around crack tips, which is important for crack propagation analysis [4].

One can mention some applications of investigating half-spaces in the framework of coupled thermoelasticity. Thermoelastic stresses are capable of producing significant lithospheric deflection [5]. A locally increased heat flow into the base of the lithosphere, produces uplift in two ways, which are vertical and horizontal heat expansion each of which affects the lithosphere. The vertical heat expansion causes a simple thickening of the lithosphere plate, while the horizontal expansion induces isostatic uplift. Also, the uneven heating of the lithosphere plate will produce thermoelastic bending moments which tend to induce local subsidence rather than uplift. Based on the results of Bills [5], the amount of uplift and subsidence

produced by a given heat source in the lithosphere of Earth depends on a number of factors including the strength, duration and lateral extent of the thermal anomaly; and the thickness, density, rigidity and viscosity of the lithosphere plate [5]. Thermally induced uplift and subsidence are recognized as a major source of large-scale topographic and structural features in both oceanic and continental regions. In particular, the gradual subsidence of oceanic plates as they move away from ridges is adequately explained in terms of conductive heat loss, leading to lithospheric densification and isostatic subsidence [5–8].

Lanzano [9] examined the problem of the thermoelastic deformation of a spherical solid like Earth with constant elastic parameters heated by a spontaneous decay of radiogenic elements. Based on his research, the two processes, radioactive cooling through the surface and radiogenic heating at the interior of planets, must entail certain mechanical consequences. Any change in the temperature profile of planetary masses must bring about a corresponding contraction or dilatation of the material. Stresses arising from heating and cooling of the planetary masses are large enough to alter even their sizes [9].

The problem of a surface/buried mechanical load in an elastic half-space (without thermal effect) has a long and interesting history for the areas of wave propagation and soil dynamics. Some of main contributions in these problems were made by Lamb [10], Love [11], Ewing et al. [12], Achenbach [13], Aki and Richards [14] and Pak [15], etc. The mathematical analysis of the problem including coupled mechanical and thermal effects (i.e. thermoelastodynamic boundary value problem; TEDBVP) would be more complicated. Because of this, TEDBVPs have received less attention than elastodynamics.

One may find a good history for linear theory of thermoelasticity and its various applications in physics and engineering in Nowinski [16]. However, we are going to mention a short related history for the problem investigated in this paper. In the framework of coupled thermoelasticity in either isotropic or anisotropic media, there exist some researches in the literature and the most important contributions in this field are probably the works done by Duhamel in 1837 (see Carlson [17]), Biot [18] in 1956, Lessen [19] in 1957, Deresiewicz [20] in 1958, Zorski [21] in 1958, Novatskii [22] in 1962, Nowacki [23–26], Verruijt [27] in 1969, Carlson [17] in 1972, Nowinski [16] in 1978, Chandrasekharaiah and Srikantiah [28,29], Chandrasekharaiah [30–32], Georgiadis et al. [33] in 1999, Ding et al. [34] in 2000, Lykotrafitis et al. [35] in 2001, Sharma [36] in 2001, Svanadze [37] in 2004, Babaei et al. [38] in 2008, Scalia and Svanadze [39] in 2009, Sheng and Wang [40] in 2010, Scalia et al. [41] in 2010, Kumar and Panchal [42] in 2011, Eskandari-Ghadi et al. [43,44], Raoofian-Naeeni et al. [45] in 2013, Youssef and El-Bary [46] in 2014 and Hayati et al. [47,48].

Duhamel was the first who presented the coupling between deformation and temperature fields of a body and introduced the partial differential equations of coupled thermoelasticity, which subsequently developed by Voigt and Jeffrey (see [23]). Although Duhamel presented equations of thermoelasticity with coupling of field of deformation with field of temperature already in 1837, only papers published 120 years later by Biot [18] of 1956 and Lessen [19] of 1957 gave a new impulse to do research in this area [49]. However, the comprehensive development in this theory based on the irreversible thermodynamics was presented in the pioneering paper of Biot, who also formulated the variational theorem of thermoelasticity [18]. In the coupled thermoelasticity theory, the deformation of a body and the distribution of its temperature are completely coupled. The description of interactions between these two physical fields can be expressed based on the first and the second laws of thermodynamics, which in the case of elastic deformations are reduced to the governing equations of coupled thermoelasticity theory [17,23]. By making an analogy between thermoelastodynamics and the theory of elasticity of porous materials, Biot [18], in terms of potential functions, presented a complete general solution for the coupled thermoelasticity in the absence of heat source and the inertia effect for isotropic media, where the completeness was shown by Verruijt [27]. Later, Qing and Wang presented a simpler proof for the completeness of Biot's solution (see [34]). Deresiewicz [20] and Zorski [21] separately presented a complete solution for thermoelasticity problems in isotropic media. Novatskii [22] investigated many dynamic problems of thermoelasticity. Nowacki, in his books [23,26], considered many dynamic problems of thermoelasticity and presented solutions of the equations of thermoelasticity and provided a vast discussion on the numerical results, graphs

and responses. Nowacki [24] determined the Green's functions for the thermoelastic medium. He also presented the completeness of stress functions in the thermoelasticity problems [25]. Chandrasekharaiah and Srikantiah [28] investigated waves of general type propagating in a compressible non-viscous liquid layer sandwiched in between two different thermoelastic half-spaces. They have found that, unlike in the case of classical waves (Stoneley-type), the motion is not necessarily two dimensional and that the particles of the solids and the liquid vibrate in three different planes in general. Chandrasekharaiah and Srikantiah [29] also investigated the edge waves in a thermoelastic plate. They employed the temperature-rate-dependent thermoelasticity theory to study waves propagating along the edges of a thin flat plate of infinite length, which is in a state of plane stress. They also derived the governing equations of the plane stress problem and have found that the speed of heat waves in their problem is in general less than that in the plane strain and the general three-dimensional problems.

Chandrasekharaiah [30] formulated the theory of micropolar thermoelasticity which includes heat flux among the constitutive variables and it has been found that the linearized version of the theory presented by [30] admits the second-sound effects. Chandrasekharaiah [31] presented a review article in the field of coupled thermoelasticity. He presented a fairly self-contained bibliographical review of the thermoelasticity literature. In his review article, novelties involved in the formulations of the theories of thermoelasticity are emphasized, and concise derivations of the governing equations are presented. By presenting an exhaustive list of references, Chandrasekharaiah [31] summarized the solutions of related initial-boundary value problems and illustrated the salient aspects of thermoelasticity theories. Chandrasekharaiah [32] studied the one-dimensional wave propagation in a half-space, by employing the linear theory of thermoelasticity without energy dissipation for homogeneous and isotropic materials. He employed the Laplace transform to solve the problem and obtained the exact solutions, in closed form, for the displacement, temperature, strain and stress fields. Georgiadis et al. [33] studied thermoelastodynamic disturbances in a half-space under the action of a buried thermal/mechanical line source. The potential functions introduced by Ding et al. [34] for general solution of coupled thermoelastic problems in the absence of body force and heat source are also worthwhile to be mentioned. Lykotrafitis et al. [35] studied three-dimensional thermoelastic wave motion under the action of both thermal and mechanical buried point sources by using the Laplace transform.

Sharma [36] investigated the propagation of thermoelastic waves in a homogeneous isotropic plate subjected to stress free and rigid insulated and isothermal conditions in the context of conventional coupled thermoelasticity. He showed that the motion for purely transverse (SH) modes gets decoupled from rest of the motion and remain unaffected due to thermomechanical coupling and thermal relaxation effects. He also obtained the phase velocities for SH waves. Svanadze [37] established the fundamental solutions of the equations of the theory of thermoelasticity with microtemperatures by means of elementary functions. Babaei et al. [38] studied the coupled thermoelasticity of functionally graded beams. They obtained the solution of Euler-Bernoulli beams subjected to lateral thermal shock loads under coupled thermoelastic (Biot's theory) assumption. They solved the the equations of motion and the conventional coupled energy equation simultaneously to obtain the transverse deflection and temperature distribution in the beam. Scalia and Svanadze [39] studied the potential method in the linear theory of thermoelasticity with microtemperatures. They investigated the basic boundary value problems of steady vibrations using the potential method. They employed the Sommerfeld–Kupradze type radiation conditions and established the basic problems of thermoelastopotentials. Sheng and Wang [40] studied thermoelastic vibration and buckling analysis of functionally graded piezoelectric cylindrical shells, where the cylindrical shell is made from a piezoelectric material having gradient change along the thickness. They solved their problem utilizing Hamilton's principle and the Maxwell equation and the first-order shear deformation theory, and taking into account both the direct and the converse piezoelectric effects to investigate the thermoelastic vibration and buckling analysis of cylindrical shell. Scalia et al. [41] presented the basic theorems in the linear equilibrium theory of thermoelasticity with microtemperatures. They obtained some basic results of the classical theories of elasticity and thermoelasticity and proved the uniqueness theorems of the internal

and external basic boundary value problems. They also presented the basic properties of thermoelastopotentials and singular integral operators. Kumar and Panchal [42] investigated the propagation of axial symmetric cylindrical surface waves in a cylindrical bore through a homogeneous isotropic thermoelastic diffusive medium of infinite extent. They used the three different theories of thermoelasticity namely, Coupled Thermoelasticity (Biot's theory), Lord and Shulman; and Green and Lindsay theories to study the problem.

Eskandari-Ghadi et al. [43] presented a complete solution including three scalar potential functions for the coupled displacement-temperature equations of motion and heat equation in the framework of Biot's coupled thermoelasticity theory, where the governing equations for the potential functions are the wave, heat or a repeated wave-heat equation. They proved the completeness of their theorem based on a retarded Newtonian potential function; existence of solutions for the repeated wave and heat equation; and perturbation theory. They proved that if no heat source exists, the number of potential functions is reduced to two, and in some special conditions, the number of potential functions is reduced to only one, and the required conditions are discussed. Also, they degenerated their thermoelastodynamic solution to elastodynamics. Raoofian-Naeeni et al. [45], in the absent of heat source, by using two scalar potential functions presented by Eskandari-Ghadi et al. [44] for thermoelastodynamic problems, and by using the correspondence principle, presented an analytical derivation of fundamental Green's functions for bi-material half-space composed of a transversely isotropic thermoelastic layer and an isotropic thermoviscoelastic half-space affected by finite surface or interfacial sources. Youssef and El-Bary [46] derived the thermoelastic material response due to laser pulse heating in context of four theorems of thermoelasticity. They studied the induced temperature and stress fields in an elastic half-space in the context of classical coupled thermoelasticity (Biot), and generalized thermoelasticity (Lord–Shulman, Green–Lindsay and Green–Naghdi) theorems in a unified system of equations.

Hayati et al. [47] with the aid of the complete scalar potential function presented by Eskandari-Ghadi et al. [43], have presented an analytical formulations for thermoelastodynamic Green's functions of an axisymmetric linear elastic isotropic half-space within the Biot's coupled thermoelasticity theory. By using the potential function, they uncoupled the governing equations of thermoelasticity into a sixth-order partial differential equation governed the potential function in cylindrical coordinate system. For solving their problem, they utilized the Hankel integral transform to suppress the radial variable. Also, Hayati et al. [48] have investigated the frequency domain analysis of an axisymmetric thermoelastic transversely isotropic half-space by using a complete scalar potential function which has been presented by Eskandari-Ghadi et al. [44] for transversely isotropic thermoelastodynamic problems.

Actually, the present study is a sequence of recent studies which have done by Hayati et al. [47] and [48]. Both of these recent studies have considered the axisymmetric problem with only the vertical traction and heat boundary conditions, while the present study considers the more general thermoelastodynamic problem with arbitrary lateral and vertical traction and heat flux boundary conditions. In this paper, by expressing the displacements and the change of temperature in terms of the potential functions as have been suggested in Eskandari-Ghadi et al. [43], the equations of motion accompanied with the heat conduction equation are reduced to two uncoupled partial differential equations, which are a sixth- and a second-order partial differential equations, governing the potential functions. By employing the Fourier expansion in terms of angular coordinate and Hankel transforms in terms of radial coordinate in cylindrical coordinate system, the angular and radial coordinates are suppressed, and thus the governing equations for potential functions are reduced to two ordinary differential equations in terms of depth, which are solved readily. Then, the displacement, temperature and stress fields are derived via the relationships among these functions and the potential functions in the Hankel–Fourier domain. Applying the inverse theorem for Hankel integral transforms, the coefficients of Fourier series are determined as improper line integrals. Because of complexity of the integrands involved in these integrals, they are numerically evaluated in this paper. To this end, a proper quadrature scheme coded in Mathematica software is used. To illustrate the physical behavior of the solutions, the numerical results are graphically depicted for

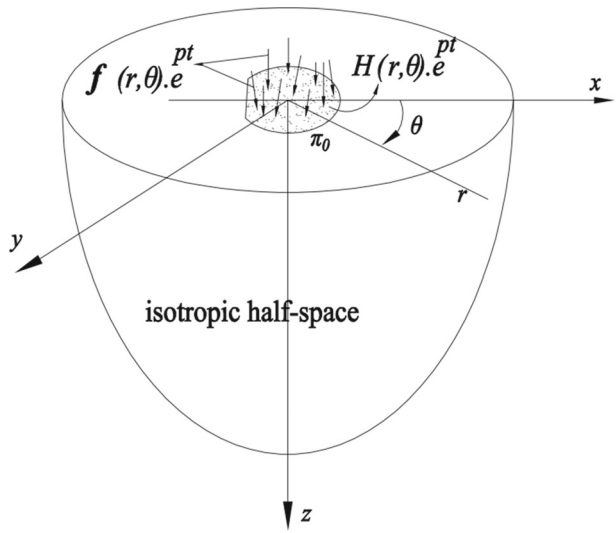

FIG. 1. A half-space subjected to an arbitrary dynamic traction with intensity $\boldsymbol{f}(r,\theta)\,e^{pt}$ and a distributed heat flux with intensity $H(r,\theta)\,e^{pt}$ on a finite region π_0 at the surface

different three cases of load and heat distributions. To prove the validity of the numerical integrations, the displacements are numerically evaluated for special elastodynamic case and compared with results presented by Pak [15], where a very good agreement is achieved. Some points are mentioned about wave propagation in thermoelastodynamic media and compared with elastodynamics. On the other hand, since the potential functions used in this paper are applicable from simple elastostatics to the complex problems of thermoelastodynamics (see [43]), it is shown that the solution derived in this paper could be analytically degenerated to specific cases reported in the literature. For example in the case of elastodynamic, the solution is degenerated to the results of Pak [15] for surface excitation and for the case of an axisymmetric quasi-static thermoelastic problem, the results are reduced to Ding et al. [34].

The general solution given in this paper could be implemented in some engineering applications such as the explosions happens on the ground surface and applied heat loadings near to the surface. In addition, this study could be applicable as kernels in the boundary element method or boundary integral formulations which may be useful in the numerical treatment of more complicated thermoelastodynamic problems involving half-space geometries.

2. Statement of the boundary value problem

A half-space containing thermoelastic isotropic material defined as $z \geq 0$ in a cylindrical coordinate system (r,θ,z) is considered to be under the effects of an external traction and a specific heat flux at the free surface $z=0$ (see Fig. 1). According to the linear theory of coupled thermoelasticity, the basic equations of problem ignoring body forces and heat supply could be expressed as follow (see [18,43])

$$\mu\nabla^2\mathbf{U} + (\lambda+\mu)\,\nabla\varepsilon - \beta\nabla T = \rho\partial^2\mathbf{U}/\partial t^2 \tag{1}$$

$$k\nabla^2 T = c\partial T/\partial t + T_0\beta\,(\partial\varepsilon/\partial t) \tag{2}$$

where $\mathbf{U}=(U_r,U_\theta,U_z)$ is the displacement vector; ρ, the mass density; ∇, the gradient operator; ∇^2, the Laplacian differential operator; $\beta=(2\mu+3\lambda)\,\alpha$, the thermal stress coefficient; α, the thermal expansion coefficient; $\varepsilon=\varepsilon_{rr}+\varepsilon_{\theta\theta}+\varepsilon_{zz}$ the dilatation; c, the specific heat; $T=T_1-T_0$, the temperature increment;

T_1, the absolute temperature; T_0, the reference temperature; k, the thermal conductivity; and λ and μ are Lame's constants. The strain–displacement relationships in the cylindrical coordinate system can be presented as follows [50]

$$\varepsilon_{rr}=\frac{\partial U_r}{\partial r},\varepsilon_{\theta\theta}=\frac{1}{r}\frac{\partial U_\theta}{\partial\theta}+\frac{U_r}{r},\varepsilon_{zz}=\frac{\partial U_z}{\partial z}, \tag{3}$$

Substituting Eq. (3) into Eqs. (1) and (2), four coupled equations of motion and energy equation are derived in terms of displacement components U_r,U_θ,U_z and temperature T as follows

$$\begin{aligned}
&(2\mu+\lambda)\left(\frac{\partial^2U_r}{\partial r^2}+\frac{\partial U_r}{r\partial r}-\frac{U_r}{r^2}\right)+\frac{\mu}{r^2}\frac{\partial^2U_r}{\partial\theta^2}+\mu\frac{\partial^2U_r}{\partial z^2}\\
&\quad+(\mu+\lambda)\left(\frac{\partial^2U_\theta}{r\partial r\partial\theta}+\frac{\partial U_\theta}{r^2\partial\theta}+\frac{\partial^2U_z}{\partial r\partial z}\right)-\frac{2(2\mu+\lambda)}{r^2}\frac{\partial U_\theta}{\partial\theta}-\beta\frac{\partial T}{\partial r}=\rho\frac{\partial^2U_r}{\partial t^2},\\
&\mu\left(\frac{\partial^2U_\theta}{\partial r^2}+\frac{\partial U_\theta}{r\partial r}-\frac{U_\theta}{r^2}\right)+\frac{(2\mu+\lambda)}{r^2}\frac{\partial^2U_\theta}{\partial\theta^2}+\mu\frac{\partial^2U_\theta}{\partial z^2}+\frac{2(2\mu+\lambda)}{r^2}\frac{\partial U_r}{\partial\theta}\\
&\quad+(\mu+\lambda)\left(\frac{\partial^2U_r}{r\partial r\partial\theta}-\frac{\partial U_r}{r^2\partial\theta}+\frac{\partial^2U_z}{r\partial\theta\partial z}\right)-\beta\frac{\partial T}{r\partial\theta}=\rho\frac{\partial^2U_\theta}{\partial t^2},\\
&\mu\left(\frac{\partial^2U_z}{\partial r^2}+\frac{\partial U_z}{r\partial r}+\frac{\partial^2U_z}{r^2\partial\theta^2}\right)+(2\mu+\lambda)\frac{\partial^2U_z}{\partial z^2}\\
&\quad+(\mu+\lambda)\left(\frac{\partial^2U_r}{\partial r\partial z}+\frac{\partial U_r}{r\partial z}+\frac{\partial^2U_\theta}{r\partial\theta\partial z}\right)-\beta\frac{\partial T}{\partial z}=\rho\frac{\partial^2U_z}{\partial t^2},\\
&-\beta T_0\frac{\partial}{\partial t}\left(\frac{\partial U_r}{\partial r}+\frac{\partial U_\theta}{r\partial\theta}\right)-\beta T_0\frac{\partial^2U_z}{\partial z\partial t}+\left(k\nabla^2-c\frac{\partial}{\partial t}\right)T=0
\end{aligned} \tag{4}$$

Assume that an arbitrary time-harmonic traction $\boldsymbol{f}(r,\theta)e^{pt}$ and a prescribed heat flux $H(r,\theta)e^{pt}$ ($p=i\omega$) to be applied on a finite patch π_0 at $z=0$ (see Fig. 1). Thus, the traction and the thermal boundary conditions may be written as

$$\begin{cases}\sigma_{rz}(r,\theta,z=0)=-P(r,\theta),\\ \sigma_{\theta z}(r,\theta,z=0)=-Q(r,\theta),(r,\theta)\in\pi_0\\ \sigma_{zz}(r,\theta,z=0)=-R(r,\theta),\\ \frac{\partial T(r,\theta,z=0)}{\partial z}=\frac{H(r,\theta)}{k}\end{cases} \tag{5}$$

$$[\sigma_{rz}=\sigma_{\theta z}=\sigma_{zz}=\partial T/\partial z](r,\theta,z=0)=0,(r,\theta)\notin\pi_0 \tag{6}$$

in which $P(r,\theta),Q(r,\theta)$ and $R(r,\theta)$ are the components of the traction vector $\boldsymbol{f}(r,\theta)$ in $r-$, $\theta-$, and $z-$ direction, respectively, and $H(r,\theta)$ is the heat flux passing in the $z-$ direction through a circular disc of radius a. Moreover, the stresses and displacements should satisfy the following regularity conditions

$$\begin{aligned}&\lim_{r\to\infty}\sigma_{ij}(r,\theta,z)=0,\lim_{r\to\infty}U_i(r,\theta,z)=0,\\&\lim_{z\to\infty}\sigma_{ij}(r,\theta,z)=0,\lim_{z\to\infty}U_i(r,\theta,z)=0\end{aligned} \tag{7}$$

3. Solutions for the boundary value problem

A common and convenient way to solve a system of coupled linear partial differential equations like Eqs. (4) is the method of potential function. Eskandari-Ghadi et al. [43] proposed a set of complete potential functions to uncouple the coupled equations of motion and energy equation for isotropic thermoelastic materials in the Cartesian coordinate system. Hayati et al. [47] in their similar problem under surface mechanical and thermal loading have used the special form of Eskandari-Ghadi et al. [43] potential

function for axisymmetric problem successfully. According to the Eskandari-Ghadi et al. [43] potential functions, the displacement- and temperature-potential relationships in the cylindrical coordinate system are written via the following relations

$$\begin{aligned}
U_r(r,\theta,z,t) &= -\frac{1}{\mu^2}\left(k(\mu+\lambda)\nabla_T^2 - \beta^2 T_0\frac{\partial}{\partial t}\right)\frac{\partial^2 F}{\partial r\partial z} - \frac{\partial \chi}{r\partial\theta},\\
U_\theta(r,\theta,z,t) &= -\frac{1}{\mu^2}\left(k(\mu+\lambda)\nabla_T^2 - \beta^2 T_0\frac{\partial}{\partial t}\right)\frac{\partial^2 F}{r\partial\theta\partial z} + \frac{\partial \chi}{\partial r},\\
U_z(r,\theta,z,t) &= \left[\frac{k}{\mu}\nabla_T^2\left(\frac{2\mu+\lambda}{\mu}\nabla_{r\theta}^2 + \frac{\partial^2}{\partial z^2} - \rho_0\frac{\partial^2}{\partial t^2}\right) - \frac{\beta^2}{\mu^2}T_0\frac{\partial}{\partial t}\nabla_{r\theta}^2\right]F,\\
T(r,\theta,z,t) &= T_0\frac{\beta}{\mu}\left(\nabla^2 - \rho_0\frac{\partial^2}{\partial t^2}\right)\frac{\partial^2 F}{\partial t\partial z},
\end{aligned} \tag{8}$$

where

$$\rho_0 = \frac{\rho}{\mu}, \nabla_{r\theta}^2 = \frac{\partial^2}{\partial r^2} + \frac{\partial}{r\partial r} + \frac{\partial^2}{r^2\partial\theta^2}, \nabla^2 = \nabla_{r\theta}^2 + \frac{\partial^2}{\partial z^2}, \nabla_T^2 = \nabla^2 - \frac{\partial}{c_T\partial t}, \frac{1}{c_T} = \frac{c}{k}. \tag{9}$$

Substituting Eqs. (8) into (4), two independent sixth- and second-order partial differential equations governing, respectively, the potential functions $F$and χ are obtained as below [43]

$$\left[k(2\mu+\lambda)\Box_T^2\Box_1^2\Box_2^2 - \beta^2 T_0\nabla^2(\partial/\partial t)\left(\nabla^2 - \rho_0\partial^2/\partial t^2\right)\right]F(r,\theta,z,t) = 0, \tag{10}$$

$$\Box_0^2\chi(r,\theta,z,t) = 0, \tag{11}$$

where

$$\Box_i^2 = \nabla^2 - \frac{\partial^2}{c_i^2\partial t^2}, (i=0,1,2), \frac{1}{c_0^2} = \rho_0, \frac{1}{c_1^2} = \frac{\rho}{2\mu+\lambda}, \frac{1}{c_2^2} = \rho_0. \tag{12}$$

The square operators ($\Box_i^2$) are defined in (12) for wave operators with different phase velocities. In addition, c_1 and c_2 are the dilatational and shear wave speeds, respectively. In the case of time-harmonic motion with a time factor e^{pt}, one can express the displacements, temperature, stresses and potential functions in the following form [51]

$$[\boldsymbol{U}, T, \boldsymbol{\sigma}, F, \chi(r,\theta,z,t)] = [\boldsymbol{u}, T, \boldsymbol{\sigma}, F, \chi(r,\theta,z)]e^{pt}, etc. \tag{13}$$

where $p = i\omega$, ω is the circular frequency of the harmonic motion and $i = \sqrt{-1}$. Substituting Eqs. (13) into (8), one can rewrite the Eq. (8) in the following form

$$\begin{aligned}
u_r(r,\theta,z) &= -\frac{\partial^2}{\partial r\partial z}\left(\Box_3^2 F\right) - \frac{\partial\chi}{r\partial\theta},\\
u_\theta(r,\theta,z) &= -\frac{\partial^2}{r\partial\theta\partial z}\left(\Box_3^2 F\right) + \frac{\partial\chi}{\partial r},\\
u_z(r,\theta,z) &= \left[\frac{k}{\mu}\hat{\Box}_T^2\left(\left(\frac{2\mu+\lambda}{\mu}\right)\nabla_{r\theta}^2 + \frac{\partial^2}{\partial z^2} - \rho_0 p^2\right) - \frac{\beta^2 T_0 p}{\mu^2}\nabla_{r\theta}^2\right]F,\\
T(r,\theta,z) &= \frac{\beta T_0 p}{\mu}\frac{\partial}{\partial z}\left(\nabla^2 - \rho_0 p^2\right)F
\end{aligned} \tag{14}$$

where

$$\begin{aligned}
\Box_3^2 &= \frac{1}{\mu^2}\left(k(\mu+\lambda)\hat{\Box}_T^2 - \beta^2 T_0 p\right),\\
\hat{\Box}_T^2 &= \nabla^2 - (p/c_T)
\end{aligned} \tag{15}$$

and u_r, u_θ and u_z are the amplitudes of the components of displacement vector in $r-$, $\theta-$, and $z-$ directions, respectively, and eventually, T is the amplitude of temperature. Also considering Eq. (13), one can rewrite the governing equations for potential functions F and χ as follow

$$\left[k\left(2\mu+\lambda\right)\hat{\square}_T^2\hat{\square}_1^2\hat{\square}_2^2-\beta^2T_0p\nabla^2\left(\nabla^2-\rho_0p^2\right)\right]\hat{F}\left(r,\theta,z\right)=0 \tag{16}$$

$$\hat{\square}_0^2\chi\left(r,\theta,z\right)=0 \tag{17}$$

where $\hat{\square}_i^2=\nabla^2-(p^2/c_i^2),(i=0,1,2)$ and $\hat{\square}_T^2$ has been defined in Eq. (15). As it can be seen in Eqs. (8),(10) and (11) or equivalently in (14),(16) and (17), the operators applied on the potential functions have been introduced in such a way that the Hankel integral transforms to be applied readily. Thus, in order to solve Eqs. (16) and (17), Fourier expansion as well as Hankel integral transforms is employed to suppress the angular and radial variables, respectively. It is clear that the Hankel integral transforms of any functions exist due to the regularity conditions in r-direction given in the relations (7). The complex Fourier expansion of potential functions F and χ, and the mth coefficients of Fourier expansions of F and χ, which are F_m and χ_m, can be defined as follows [52]

$$\begin{aligned}\left[F,\chi\left(r,\theta,z\right)\right]&=\sum_{m=-\infty}^{+\infty}\left[F_m,\chi_m\left(r,z\right)\right]e^{\mathrm{i}m\theta},\\ \left[F_m,\chi_m\left(r,z\right)\right]&=\frac{1}{2\pi}\int_0^{2\pi}\left[F,\chi\left(r,\theta,z\right)\right]e^{-\mathrm{i}m\theta}\mathrm{d}\theta.\end{aligned} \tag{18}$$

The mth-order Hankel integral transforms of $[F_m,\chi_m(r,z)]$ which denoted as $[\tilde{F}_m^m,\tilde{\chi}_m^m(\xi,z)]$ and the inverse Hankel transforms of $[\tilde{F}_m^m,\tilde{\chi}_m^m(\xi,z)]$ are defined as below [52]

$$\begin{aligned}\left[\tilde{F}_m^m,\tilde{\chi}_m^m\left(\xi,z\right)\right]&=\int_0^\infty rJ_{\mathrm{m}}\left(\xi r\right)\left[F_m,\chi_m\left(r,z\right)\right]\mathrm{d}r,\\ \left[F_m,\chi_m\left(r,z\right)\right]&=\int_0^\infty \xi J_{\mathrm{m}}\left(\xi r\right)\left[\tilde{F}_m^m,\tilde{\chi}_m^m\left(\xi,z\right)\right]\mathrm{d}\xi.\end{aligned} \tag{19}$$

where ξ is the parameter of Hankel integral transform and J_{m} denotes the Bessel function of the first kind and mth order. Similar expressions for the displacement, temperature difference and stress components can be written. With the use of Fourier expansion and the Hankel integral transforms as defined in (18) and (19), one can write Eqs. (16) and (17) in the form of the following ordinary differential equations with respect to z

$$\left(\partial^6+I_3\left(\xi\right)\partial^4+I_2\left(\xi\right)\partial^2+I_1\left(\xi\right)\right)\tilde{F}_m^m\left(\xi,z\right)=0 \tag{20}$$

$$\left(\partial^2+I_0\left(\xi\right)\right)\tilde{\chi}_m^m\left(\xi,z\right)=0 \tag{21}$$

where $\partial^n=\mathrm{d}^n/\mathrm{d}z^n$ and

$$\begin{aligned}I_3\left(\xi\right)&=\alpha_1-3\xi^2-\beta^2T_0p/\left(k\left(2\mu+\lambda\right)\right),\\ I_2\left(\xi\right)&=\alpha_2-2\alpha_1\xi^2+3\xi^4-\beta^2T_0p\left(\alpha_3-2\xi^2\right)/\left(k\left(2\mu+\lambda\right)\right),\\ I_1\left(\xi\right)&=\alpha_4-\alpha_2\xi^2+\alpha_1\xi^4-\xi^6-\beta^2T_0p\left(\xi^4-\alpha_3\xi^2\right)/\left(k\left(2\mu+\lambda\right)\right),\\ I_0\left(\xi\right)&=-\left(\xi^2+\rho_0p^2\right).\end{aligned} \tag{22}$$

In addition

$$\alpha_1 = -p\left(\frac{c}{k} + \frac{p\rho}{\mu} + \frac{p\rho}{2\mu+\lambda}\right),$$
$$\alpha_2 = \frac{p^3\rho\left[(3\mu+\lambda)c + p\rho k\right]}{\mu k\left(2\mu+\lambda\right)},$$
$$\alpha_3 = -\rho_0 p^2, \quad \alpha_4 = \frac{-p^5\rho^2 c}{\mu k\left(2\mu+\lambda\right)}. \tag{23}$$

The solutions for the Eqs. (20) and (21) are given by

$$\tilde{F}_m^m(\xi,z) = A_m(\xi)e^{-\lambda_1 z} + B_m(\xi)e^{-\lambda_2 z} + C_m(\xi)e^{-\lambda_3 z} + E_m(\xi)e^{\lambda_1 z} + G_m(\xi)e^{\lambda_2 z} + H_m(\xi)e^{\lambda_3 z} \tag{24}$$
$$\tilde{\chi}_m^m(\xi,z) = D_m(\xi)e^{-\lambda_4 z} + L_m(\xi)e^{\lambda_4 z} \tag{25}$$

where A_m to L_m are some unknown functions to be determined with the use of boundary conditions. In addition, $\lambda_4 = \sqrt{\xi^2+\rho_0 p^2}$ and $\pm\lambda_i, (i=1,2,3)$ are the roots of the following polynomial equation which is the characteristic differential equation of Eq. (20)

$$\lambda^6 + I_3(\xi)\lambda^4 + I_2(\xi)\lambda^2 + I_1(\xi) = 0 \tag{26}$$

$\lambda_i, (i = 1\,\text{to}\,4)$ are defined in such a way that their real parts to be positive. In addition, $\lambda_i, (i=1,2,3)$ could be expressed as below

$$\lambda_1 = \sqrt{b_1\left(b_2 - p\sqrt{b_3}\right)}, \lambda_2 = \sqrt{\xi^2+\rho_0 p^2}, \lambda_3 = \sqrt{b_1\left(b_2 + p\sqrt{b_3}\right)} \tag{27}$$

where

$$b_1 = 1/\left(2k\left(2\mu+\lambda\right)\right), \quad b_2 = \left(2\mu+\lambda\right)\left(pc+2k\xi^2\right) + p\left(kp\rho+\beta^2 T_0\right),$$
$$b_3 = \beta^4 T_0^2 + \left(c\left(2\mu+\lambda\right) - kp\rho\right)^2 + 2\beta^2 T_0\left(c\left(2\mu+\lambda\right) + kp\rho\right). \tag{28}$$

From Eq. (27), it can be seen that the functions $\lambda_i, (i=1-4)$ are multi-valued functions [53]. These functions have some branch points, which may be located on the common path of integration, which is the positive part of real axis in complex $\xi-$ plane. The branch points $\xi_{\lambda_i}, (i=1-4)$ can be determined by solving equations $\lambda_i(\xi) = 0, (i=1-4)$ as follows

$$\xi_{\lambda_1} = \pm\sqrt{b_1\left(k\rho\omega^2 + i\left(-b_4 + \omega\sqrt{ib_5+b_6}\right)\right)},$$
$$\xi_{\lambda_2} = \xi_{\lambda_4} = \pm\omega\sqrt{\rho/\mu},$$
$$\xi_{\lambda_3} = \pm\sqrt{b_1\left(k\rho\omega^2 + i\left(-b_4 - \omega\sqrt{ib_5+b_6}\right)\right)} \tag{29}$$

where

$$b_4 = \omega\left(c\left(2\mu+\lambda\right) + \beta^2 T_0\right),$$
$$b_5 = 2k\rho\omega\left(\beta^2 T_0 - c\left(2\mu+\lambda\right)\right),$$
$$b_6 = \left(\beta^2 T_0 + c\left(2\mu+\lambda\right)\right)^2 - \left(k\rho\omega\right)^2 \tag{30}$$

In the Hankel integral transforms, the range of integration is $\xi \in [0,+\infty)$ and thus the path of integration in the inverse Hankel integral transforms is the positive real line. Therefore, we should pay attention to those branch points $\xi_{\lambda_i}, (i=1-4)$ with the positive real parts, when we need to inverse the Hankel integral transforms. According to Eq. (29), both branch points ξ_{λ_1} and ξ_{λ_3} are conjugate complex numbers and they have non-zero imaginary parts, so they are not located on the path of integration (real axis in complex ξ-plane), but the branch points $\xi_{\lambda_2} = \xi_{\lambda_4}$ are pure real numbers and thus are located on

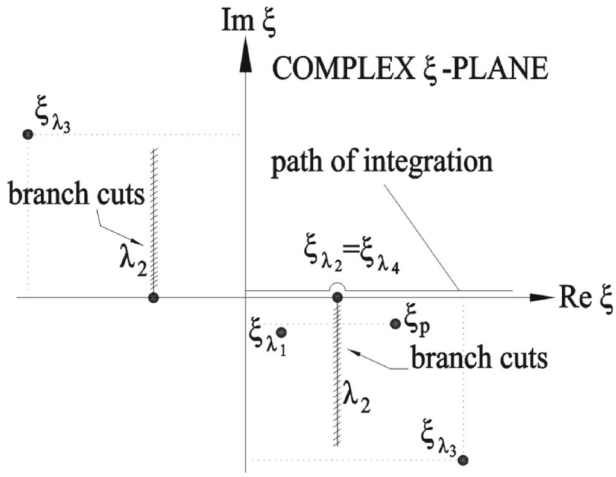

FIG. 2. Common path of integration and branch cuts, branch points and poles

the path of integration. Based on Eq. (29), the branch points ξ_{λ_2} and ξ_{λ_4} are, respectively, corresponds to the shear wave numbers horizontally (SH) and vertically (SV) polarized, while the branch points ξ_{λ_1} and ξ_{λ_3} are related to coupled compression (P) and thermal wave numbers (see [45]). As can be seen, the shear waves are not affected by thermal coupling, however contrary to elastodynamics, here the dilatational wave number undergoes some damping and dispersion due to thermomechanical coupling. To be consistent with the Eqs. (24) and (25), we should define a Riemann surface with two sheets such that $\lambda_i, (i = 2, 4)$ be single valued and analytically continuous from one sheet to another. This can be obtained by defining the branch cuts for $\lambda_2 = \lambda_4$ on the complex ξ- plane as shown in Fig. 2 with branch points emanating from $\xi_{\lambda_2} = \xi_{\lambda_4}$ such that the real parts of $\lambda_2 = \lambda_4$ are always non-negative (see e. g. [15,54]). If we assume that the thermal stress coefficient β is very small (it may approach zero), so the branch points are reduced to $\xi_{\lambda_1} = \omega/c_1$ and $\xi_{\lambda_2} = \xi_{\lambda_4} = \omega/c_2$ which are the compression and shear wave numbers in elastodynamics, which reported by Pak [15] and $\xi_{\lambda_3} = \sqrt{-ic\omega/k}$ which is related to uncoupled thermal wave number.

Under this choice of the branch cuts, $e^{\lambda_i z}, (i = 1 - 4)$ terms become inadmissible due to the radiation conditions and are thus omitted from Eqs. (24) and (25), which means that $E_m = G_m = H_m = L_m = 0$. To use the solutions presented in Eqs. (24) and (25), we need to write the traction and heat flux boundary conditions and also the displacements, stresses and temperature in the Hankel–Fourier space. In addition, the boundary conditions, and the relations between the potential functions and physical functions namely displacements, stresses and temperatures should be presented in Fourier–Hankel space. Thus, after some algebraic manipulations, one may write

$$\begin{cases} \tilde{\sigma}^{m-1}_{rzm}(\xi, z=0) - i\tilde{\sigma}^{m-1}_{\theta zm}(\xi, z=0) = -\left(\tilde{P}^{m-1}_{m}(\xi) - i\tilde{Q}^{m-1}_{m}(\xi)\right), & (a) \\ \tilde{\sigma}^{m+1}_{rzm}(\xi, z=0) + i\tilde{\sigma}^{m+1}_{\theta zm}(\xi, z=0) = -\left(\tilde{P}^{m+1}_{m}(\xi) + i\tilde{Q}^{m+1}_{m}(\xi)\right), & (b) \\ \tilde{\sigma}^{m}_{zzm}(\xi, z=0) = -\tilde{R}^{m}_{m}(\xi), & (c) \\ \frac{\partial \tilde{T}^{m}_{m}}{\partial z}(\xi, z=0) = \frac{\tilde{H}^{m}_{m}(\xi)}{k} & (d) \end{cases} \tag{31}$$

$$\begin{aligned} &\tilde{u}^{m-1}_{rm} - i\tilde{u}^{m-1}_{\theta m} = -\left[g_1\partial^3 + h_1\partial\right]\tilde{F}^{m}_{m} - i\xi\tilde{\chi}^{m}_{m}, \\ &\tilde{u}^{m+1}_{rm} + i\tilde{u}^{m+1}_{\theta m} = \left[g_1\partial^3 + h_1\partial\right]\tilde{F}^{m}_{m} - i\xi\tilde{\chi}^{m}_{m}, \\ &\tilde{u}^{m}_{zm} = \left[g_2\partial^4 + h_2\partial^2 + l_2\right]\tilde{F}^{m}_{m}, \\ &\tilde{T}^{m}_{m} = \left[g_3\partial^3 + h_3\partial\right]\tilde{F}^{m}_{m} \end{aligned} \tag{32}$$

With the use of the stress-strain-temperature and the strain–displacement relationships, one can derive the stress components in terms of displacement and temperature components. Then, transferring the resulted stress components into the Fourier–Hankel transformed domain, we can obtain the stress components in terms of transformed potential functions $\tilde{F}_m^m$ and $\tilde{\chi}_m^m$ as below

$$\begin{aligned}\tilde{\sigma}_{rzm}^{m-1} - i\tilde{\sigma}_{\theta zm}^{m-1} &= -\left[g_4\partial^4 + h_4\partial^2 + l_4\right]\tilde{F}_m^m + \left[g_6\partial\right]\tilde{\chi}_m^m,\\ \tilde{\sigma}_{rzm}^{m+1} + i\tilde{\sigma}_{\theta zm}^{m+1} &= \left[g_4\partial^4 + h_4\partial^2 + l_4\right]\tilde{F}_m^m + \left[g_6\partial\right]\tilde{\chi}_m^m,\\ \tilde{\sigma}_{zzm}^{m} &= \left[g_5\partial^5 + h_5\partial^3 + l_5\partial\right]\tilde{F}_m^m\end{aligned} \tag{33}$$

where $\tilde{u}_{im}^n(\xi,z)$ and $\tilde{\sigma}_{izm}^n(\xi,z)$ for $(i=r,\theta,z)$ in Eqs. (32) and (33) are the nth-order Hankel integral transforms of the mth coefficients of the Fourier series of u_i and σ_{iz}. In addition, $\tilde{T}_m^m(\xi,z)$ has the same definition for T. The functions g_i, h_i and l_i in Eqs. (32) and (33) are defined as below

$$\begin{aligned}g_1 &= \frac{\xi k(\mu+\lambda)}{\mu^2}, h_1 = \frac{-\xi}{\mu^2}\left[k(\mu+\lambda)\left(\xi^2+\frac{pc}{k}\right)+\beta^2 T_0 p\right],\\ g_2 &= \frac{k}{\mu}, h_2 = \frac{-k}{\mu}\left[\rho_0 p^2 + \left(\xi^2+\frac{pc}{k}\right)+\xi^2\left(\frac{2\mu+\lambda}{\mu}\right)\right],\\ l_2 &= \frac{k}{\mu}\left(\xi^2+\frac{pc}{k}\right)\left(\xi^2\left(\frac{2\mu+\lambda}{\mu}\right)+\rho_0 p^2\right)+\frac{\beta^2 T_0 p\xi^2}{\mu^2},\\ g_3 &= \frac{\beta T_0 p}{\mu}, h_3 = -g_3\left(\xi^2+\rho_0 p^2\right), g_4 = \mu\left(g_1 - \xi g_2\right),\\ h_4 &= \mu\left(h_1 - \xi h_2\right), l_4 = -\mu\xi l_2, g_5 = (2\mu+\lambda)g_2, g_6 = -\mu\xi i,\\ h_5 &= \lambda\xi g_1 + (2\mu+\lambda)h_2 - \beta g_3, l_5 = \lambda\xi h_1 + (2\mu+\lambda)l_2 - \beta h_3\end{aligned} \tag{34}$$

Substituting the functions $\tilde{F}_m^m$ and $\tilde{\chi}_m^m$ from Eqs. (24) and (25) into the Eqs. (33) and $(32)_4$ and using the boundary conditions (31), results in four algebraic equations for the unknown functions A_m, B_m, C_m and D_m, which in the matrix form can be expressed as follows

$$\begin{bmatrix} -x_1 & -x_2 & -x_3 & x_4\\ x_1 & x_2 & x_3 & x_4\\ y_1 & y_2 & y_3 & 0\\ z_1 & z_2 & z_3 & 0\end{bmatrix}\begin{Bmatrix} A_m\\ B_m\\ C_m\\ D_m\end{Bmatrix} = \begin{Bmatrix} X_m\\ Y_m\\ Z_m\\ W_m\end{Bmatrix} \tag{35}$$

where in Eq. (35)we have

$$\begin{aligned}x_i &= \left[g_4\lambda_i^4 + h_4\lambda_i^2 + l_4\right], (i=1,2,3), x_4 = -g_6\lambda_4,\\ y_i &= -\left[g_5\lambda_i^5 + h_5\lambda_i^3 + l_5\lambda_i\right], (i=1,2,3),\\ z_i &= \left[g_3\lambda_i^4 + h_3\lambda_i^2\right], (i=1,2,3)\end{aligned} \tag{36}$$

and

$$X_m = -\left(\tilde{P}_m^{m-1} - i\tilde{Q}_m^{m-1}\right), Y_m = -\left(\tilde{P}_m^{m+1} + i\tilde{Q}_m^{m+1}\right), Z_m = -\tilde{R}_m^m, W_m = \tilde{H}_m^m/k \tag{37}$$

Solving the system of linear algebraic equations (35) for unknown functions $A_m, ..., D_m$, these functions can be obtained as below

$$\begin{aligned}
A_m &= \frac{1}{h(\xi)}\left[2W_m(x_3y_2 - x_2y_3) + (X_m - Y_m)(y_2z_3 - y_3z_2) + 2Z_m(x_2z_3 - x_3z_2)\right],\\
B_m &= \frac{1}{h(\xi)}\left[2W_m(x_1y_3 - x_3y_1) + (X_m - Y_m)(y_3z_1 - y_1z_3) + 2Z_m(x_3z_1 - x_1z_3)\right],\\
C_m &= \frac{1}{h(\xi)}\left[2W_m(x_2y_1 - x_1y_2) + (X_m - Y_m)(y_1z_2 - y_2z_1) + 2Z_m(x_1z_2 - x_2z_1)\right],\\
D_m &= \frac{X_m + Y_m}{2x_4}, h(\xi) = 2\left[z_1(x_3y_2 - x_2y_3) + z_2(x_1y_3 - x_3y_1) + z_3(x_2y_1 - x_1y_2)\right]
\end{aligned} \tag{38}$$

Substituting $A_m(\xi), ..., D_m(\xi)$ from Eq. (38) into Eqs. (24) and (25), and paying attention to $E_m = G_m = H_m = L_m = 0$, the functions $\tilde{F}_m^m$ and $\tilde{\chi}_m^m$ are determined. Replacing these functions into Eqs. (32), the displacement components and temperature can be obtained in the Fourier-Hankel transformed domain. Then, using the theorem of inverse Hankel integral transforms, the displacements and temperature are derived in Fourier space as below

$$\begin{aligned}
u_{rm}(r,z) &= \frac{1}{2}\int_0^\infty \{\xi\left[J_{m+1}(\xi r) - J_{m-1}(\xi r)\right]\left[g_1\partial^3 + h_1\partial\right]\left[A_m e^{-\lambda_1 z} + B_m e^{-\lambda_2 z} + C_m e^{-\lambda_3 z}\right]\\
&\quad - i\xi^2\left[J_{m+1}(\xi r) + J_{m-1}(\xi r)\right]\left[D_m e^{-\lambda_4 z}\right]\}\,\mathrm{d}\xi,\\
u_{\theta m}(r,z) &= \frac{1}{2i}\int_0^\infty \{\xi\left[J_{m+1}(\xi r) + J_{m-1}(\xi r)\right]\left[g_1\partial^3 + h_1\partial\right]\left[A_m e^{-\lambda_1 z} + B_m e^{-\lambda_2 z} + C_m e^{-\lambda_3 z}\right]\\
&\quad - i\xi^2\left[J_{m+1}(\xi r) - J_{m-1}(\xi r)\right]\left[D_m e^{-\lambda_4 z}\right]\}\,\mathrm{d}\xi,\\
u_{zm}(r,z) &= \int_0^\infty \xi J_{\mathrm{m}}(\xi r)\left[g_2\partial^4 + h_2\partial^2 + l_2\right]\left[A_m e^{-\lambda_1 z} + B_m e^{-\lambda_2 z} + C_m e^{-\lambda_3 z}\right]\mathrm{d}\xi,\\
T_m(r,z) &= \int_0^\infty \xi J_{\mathrm{m}}(\xi r)\left[g_3\partial^3 + h_3\partial\right]\left[A_m e^{-\lambda_1 z} + B_m e^{-\lambda_2 z} + C_m e^{-\lambda_3 z}\right]\mathrm{d}\xi,
\end{aligned} \tag{39}$$

With the similar procedure, we can obtain the mth coefficients of Fourier series of stress components applied on a horizontal plane with the use of the inverse Hankel integral transforms into Eqs. (33) as follows

$$\begin{aligned}
\sigma_{rzm}(r,z) &= \frac{1}{2}\int_0^\infty \xi\{\left[J_{m+1}(\xi r) - J_{m-1}(\xi r)\right]\left[g_4\partial^4 + h_4\partial^2 + l_4\right]\left[A_m e^{-\lambda_1 z} + B_m e^{-\lambda_2 z} + C_m e^{-\lambda_3 z}\right]\\
&\quad + \left[J_{m+1}(\xi r) + J_{m-1}(\xi r)\right]\left[g_6\partial\right]\left[D_m e^{-\lambda_4 z}\right]\}\,\mathrm{d}\xi,\\
\sigma_{\theta zm}(r,z) &= \frac{1}{2i}\int_0^\infty \xi\{\left[J_{m+1}(\xi r) + J_{m-1}(\xi r)\right]\left[g_4\partial^4 + h_4\partial^2 + l_4\right]\left[A_m e^{-\lambda_1 z} + B_m e^{-\lambda_2 z} + C_m e^{-\lambda_3 z}\right]\\
&\quad + \left[J_{m+1}(\xi r) - J_{m-1}(\xi r)\right]\left[g_6\partial\right]\left[D_m e^{-\lambda_4 z}\right]\}\,\mathrm{d}\xi,\\
\sigma_{zzm}(r,z) &= \int_0^\infty \xi J_{\mathrm{m}}(\xi r)\left[g_5\partial^5 + h_5\partial^3 + l_5\partial\right]\left[A_m e^{-\lambda_1 z} + B_m e^{-\lambda_2 z} + C_m e^{-\lambda_3 z}\right]\mathrm{d}\xi
\end{aligned} \tag{40}$$

On substituting Eqs. (39) and (40) into the relevant Fourier series with respect to θ, the amplitudes of displacements, stresses and temperature are obtained as

$$[u_j, \sigma_{jz}, T(r,\theta,z)] = \sum_{m=-\infty}^{+\infty} [u_{jm}, \sigma_{jzm}, T_m(r,z)]\, e^{\mathrm{im}\theta}, (j = r,\theta,z) \tag{41}$$

These functions can be derived in physical time domain as

$$[U_j, \sigma_{jz}, T(r,\theta,z,t)] = [u_j, \sigma_{jz}, T(r,\theta,z)]\, e^{pt}, (j = r,\theta,z) \tag{42}$$

4. Results for specific load and heat flux distributions

In the previous sections, the patch π_0, the mechanical load and the heat flux have been left arbitrary. In this section, the attention will be focused on the case where π_0 is a circular region and the mechanical load and the heat flux are uniformly distributed on it. Therefore, the results obtained in previous section are specified for three different cases, which are (1): a uniform vertical patch load of unit resultant, (2): a uniform horizontal patch load of unit resultant and (3): a constant heat flux.

Case (i): *A uniform vertical patch load of unit resultant.* For the case of a uniform vertical patch load of unit resultant applied on a circular patch of radius a, which is an axisymmetric case, the components of traction and heat flux are as follows

$$\begin{cases} [P,Q,R,H](r,\theta,t) = \left[0,0,\frac{1}{\pi a^2},0\right] e^{pt}, (r,\theta) \in \pi_0, \\ \pi_0 = \{(r,\theta,z)\,|0 \le \theta < 2\pi, 0 \le r \le a, z = 0\} \end{cases} \tag{43}$$

So the Fourier expansion coefficients for traction and heat flux are as follows

$$\begin{cases} P_m(r) = Q_m(r) = H_m(r) = 0 & \forall\ m, \\ R_0(r) = 1/(\pi a^2), for\ r \le a, R_0(r) = 0, & for\ r > a \\ R_m(r) = 0. & \text{for m } \neq 0 \end{cases} \tag{44}$$

and X_m, Y_m, Z_m and W_m are determined from (37) as

$$\begin{cases} X_m = Y_m = W_m = 0 & \forall m, \\ Z_{m=0} = \frac{-J_1(\xi a)}{\pi a \xi}, & Z_{m\neq 0} = 0 \end{cases} \tag{45}$$

Substituting Eqs. (45) into (38) results in

$$\begin{aligned} A_{0(vl)}(\xi) &= \frac{-2J_1(\xi a)}{\pi a \xi \times h(\xi)}(x_2 z_3 - x_3 z_2), \\ B_{0(vl)}(\xi) &= \frac{-2J_1(\xi a)}{\pi a \xi \times h(\xi)}(x_3 z_1 - x_1 z_3), \\ C_{0(vl)}(\xi) &= \frac{-2J_1(\xi a)}{\pi a \xi \times h(\xi)}(x_1 z_2 - x_2 z_1), \\ A_m = B_m &= C_m = 0\ for\ m \neq 0, \\ D_m &= 0 \quad \forall m \end{aligned} \tag{46}$$

In Eq. (46), the subscript vl is used for the Case (i), where a vertical load is applied on the surface of the half-space. Substituting Eq. (46) into Eqs. (39) and (40) and replacing the results into Eq. (41), the following displacements, temperature and normal stress are resulted as

$$
\begin{aligned}
u_{r(vl)}(r,\theta,z) &= \int_0^\infty \xi J_1(\xi r)\left[g_1\partial^3 + h_1\partial\right]\left[A_{0(vl)}e^{-\lambda_1 z} + B_{0(vl)}e^{-\lambda_2 z} + C_{0(vl)}e^{-\lambda_3 z}\right]\mathrm{d}\xi,\\
u_{\theta(vl)}(r,\theta,z) &= 0,\\
u_{z(vl)}(r,\theta,z) &= \int_0^\infty \xi J_0(\xi r)\left[g_2\partial^4 + h_2\partial^2 + l_2\right]\left[A_{0(vl)}e^{-\lambda_1 z} + B_{0(vl)}e^{-\lambda_2 z} + C_{0(vl)}e^{-\lambda_3 z}\right]\mathrm{d}\xi,\\
T_{(vl)}(r,\theta,z) &= \int_0^\infty \xi J_0(\xi r)\left[g_3\partial^3 + h_3\partial\right]\left[A_{0(vl)}e^{-\lambda_1 z} + B_{0(vl)}e^{-\lambda_2 z} + C_{0(vl)}e^{-\lambda_3 z}\right]\mathrm{d}\xi,\\
\sigma_{zz(vl)}(r,\theta,z) &= \int_0^\infty \xi J_0(\xi r)\left[g_5\partial^5 + h_5\partial^3 + l_5\partial\right]\left[A_{0(vl)}e^{-\lambda_1 z} + B_{0(vl)}e^{-\lambda_2 z} + C_{0(vl)}e^{-\lambda_3 z}\right]\mathrm{d}\xi
\end{aligned}
\tag{47}
$$

Case (ii): *A uniform horizontal patch load of unit resultant.* The components of surface traction and heat flux for the case of a uniform lateral patch load of unit resultant applied on a circular disc of radius a acting in the x-direction, which is an asymmetric case, are as follows

$$
\begin{cases}
[P,Q,R,H(r,\theta,t)] = \left(\frac{\cos\theta}{\pi a^2}, \frac{-\sin\theta}{\pi a^2}, 0, 0\right) e^{pt}, (r,\theta) \in \pi_0,\\
\pi_0 = \{(r,\theta,z)\,|0 \le \theta < 2\pi, r \le a, z = 0\}
\end{cases}
\tag{48}
$$

Thus, the Fourier expansion coefficients for traction and heat flux are as follows

$$
\begin{cases}
P_1(r) = P_{-1}(r) = 1/(2\pi a^2), & r \le a;\\
P_1(r) = P_{-1}(r) = 0, & r > a;\\
P_m(r) = 0, & \text{for m} \neq \pm 1;
\end{cases}
$$

$$
\begin{cases}
Q_1(r) = -Q_{-1}(r) = i/(2\pi a^2), & r \le a;\\
Q_1(r) = Q_{-1}(r) = 0, & r > a;\\
Q_m(r) = 0, & \text{for m} \neq \pm 1;
\end{cases}
\tag{49}
$$

$$
R_m(r) = H_m(r) = 0, \quad \forall m
$$

In addition, X_m, Y_m, Z_m and W_m are determined as

$$
\begin{aligned}
&X_{m=1} = \tfrac{-J_1(\xi a)}{\pi a \xi}, \quad X_{m\neq 1} = 0,\\
&Y_{m=-1} = \tfrac{-J_1(\xi a)}{\pi a \xi}, \quad Y_{m\neq -1} = 0,\\
&Z_m = W_m = 0, \quad \forall m
\end{aligned}
\tag{50}
$$

Substituting Eqs. (50) into (38) results in

$$
\begin{aligned}
A_{1(hl)}(\xi) &= \frac{-J_1(\xi a)}{\pi a \xi \times h(\xi)}\left(y_2 z_3 - y_3 z_2\right),\\
B_{1(hl)}(\xi) &= \frac{-J_1(\xi a)}{\pi a \xi \times h(\xi)}\left(y_3 z_1 - y_1 z_3\right),\\
C_{1(hl)}(\xi) &= \frac{-J_1(\xi a)}{\pi a \xi \times h(\xi)}\left(y_1 z_2 - y_2 z_1\right),\\
D_{1(hl)}(\xi) &= \frac{-J_1(\xi a)}{\pi a \xi \times (2x_4)},\\
&A_{-1} = -A_1, \quad B_{-1} = -B_1, \quad C_{-1} = -C_1, \quad D_{-1} = D_1,\\
&A_m = B_m = C_m = D_m = 0 \text{ for } m \neq \pm 1
\end{aligned}
\tag{51}
$$

where in Eq. (51) the subscript hl is used for the case of a horizontal load applied on the surface of the half-space. Substituting Eq. (51) into Eqs. (39) and (40) and replacing the results into Eq. (41), results in the following displacements, temperature and shear stress

$$
\begin{aligned}
u_{r(hl)}(r,\theta,z) &= \cos\theta \int_0^\infty \left\{\xi\left[J_2(\xi r) - J_0(\xi r)\right]\left[g_1\partial^3 + h_1\partial\right]\right. \\
&\quad \times \left[A_{1(hl)}e^{-\lambda_1 z} + B_{1(hl)}e^{-\lambda_2 z} + C_{1(hl)}e^{-\lambda_3 z}\right] - i\xi^2\left[J_2(\xi r) + J_0(\xi r)\right]\left[D_{1(hl)}e^{-\lambda_4 z}\right]\Big\}\,\mathrm{d}\xi, \\
u_{\theta(hl)}(r,\theta,z) &= \sin\theta \int_0^\infty \left\{\xi\left[J_2(\xi r) + J_0(\xi r)\right]\left[g_1\partial^3 + h_1\partial\right]\right. \\
&\quad \times \left[A_{1(hl)}e^{-\lambda_1 z} + B_{1(hl)}e^{-\lambda_2 z} + C_{1(hl)}e^{-\lambda_3 z}\right] - i\xi^2\left[J_2(\xi r) - J_0(\xi r)\right]\left[D_{1(hl)}e^{-\lambda_4 z}\right]\Big\}\,\mathrm{d}\xi, \\
u_{z(hl)}(r,\theta,z) &= 2\cos\theta \int_0^\infty \xi J_1(\xi r)\left[g_2\partial^4 + h_2\partial^2 + l_2\right]\left[A_{1(hl)}e^{-\lambda_1 z} + B_{1(hl)}e^{-\lambda_2 z} + C_{1(hl)}e^{-\lambda_3 z}\right]\mathrm{d}\xi, \\
T_{(hl)}(r,\theta,z) &= 2\cos\theta \int_0^\infty \xi J_1(\xi r)\left[g_3\partial^3 + h_3\partial\right]\left[A_{1(hl)}e^{-\lambda_1 z} + B_{1(hl)}e^{-\lambda_2 z} + C_{1(hl)}e^{-\lambda_3 z}\right]\mathrm{d}\xi, \\
\sigma_{rz(hl)}(r,\theta,z) &= \cos\theta \int_0^\infty \xi\left\{\left[J_2(\xi r) - J_0(\xi r)\right]\left[g_4\partial^4 + h_4\partial^2 + l_4\right]\right. \\
&\quad \times \left[A_{1(hl)}e^{-\lambda_1 z} + B_{1(hl)}e^{-\lambda_2 z} + C_{1(hl)}e^{-\lambda_3 z}\right] + \left[J_2(\xi r) + J_0(\xi r)\right]\left[g_6\partial\right]\left[D_{1(hl)}e^{-\lambda_4 z}\right]\Big\}\,\mathrm{d}\xi
\end{aligned}
\tag{52}
$$

Case (iii): *A constant heat flux.* For the case of a constant heat flux (q_0) passing through a circular patch of radius a, one may write

$$
[P, Q, R, H(r,\theta,t)] = (0,0,0,q_0)\,e^{pt}, (r,\theta) \in \pi_0 \tag{53}
$$

which results in

$$
\begin{cases}
P_m(r) = Q_m(r) = R_m(r) = 0 \quad \forall m, \\
H_0(r) = q_0, \quad r \le a; \\
H_0(r) = 0, \quad r > a; \\
H_{m\neq 0}(r) = 0
\end{cases}
\tag{54}
$$

And X_m, Y_m, Z_m and W_m are determined as

$$
\begin{aligned}
&X_m = Y_m = Z_m = 0, \quad \forall m \\
&W_{m=0} = \tfrac{aq_0 J_1(\xi a)}{k\xi}, \qquad W_{m\neq 0} = 0
\end{aligned}
\tag{55}
$$

Substituting Eqs. (55) into (38) results in

$$
\begin{aligned}
A_{0(hf)}(\xi) &= \frac{2aq_0 J_1(\xi a)}{k\xi \times h(\xi)}\left(x_3 y_2 - x_2 y_3\right), \\
B_{0(hf)}(\xi) &= \frac{2aq_0 J_1(\xi a)}{k\xi \times h(\xi)}\left(x_1 y_3 - x_3 y_1\right), \\
C_{0(hf)}(\xi) &= \frac{2aq_0 J_1(\xi a)}{k\xi \times h(\xi)}\left(x_2 y_1 - x_1 y_2\right), \\
A_m &= B_m = C_m = 0 \text{ for } m \neq 0, \\
D_m &= 0 \quad \forall m
\end{aligned}
\tag{56}
$$

where in Eq. (56) the subscript hf is used for the case of a heat flux applied on the surface of the half-space. Substituting Eq. (56) into Eqs. (39) and (40) and replacing the results into Eq. (41), results in the following displacements, temperature and normal stress

$$
\begin{aligned}
u_{r(hf)}(r,\theta,z) &= \int_0^\infty \xi J_1(\xi r)\left[g_1\partial^3 + h_1\partial\right]\left[A_{0(hf)}e^{-\lambda_1 z} + B_{0(hf)}e^{-\lambda_2 z} + C_{0(hf)}e^{-\lambda_3 z}\right]\mathrm{d}\xi,\\
u_{\theta(hf)}(r,\theta,z) &= 0,\\
u_{z(hf)}(r,\theta,z) &= \int_0^\infty \xi J_0(\xi r)\left[g_2\partial^4 + h_2\partial^2 + l_2\right]\left[A_{0(hf)}e^{-\lambda_1 z} + B_{0(hf)}e^{-\lambda_2 z} + C_{0(hf)}e^{-\lambda_3 z}\right]\mathrm{d}\xi,\\
T_{(hf)}(r,\theta,z) &= \int_0^\infty \xi J_0(\xi r)\left[g_3\partial^3 + h_3\partial\right]\left[A_{0(hf)}e^{-\lambda_1 z} + B_{0(hf)}e^{-\lambda_2 z} + C_{0(hf)}e^{-\lambda_3 z}\right]\mathrm{d}\xi,\\
\sigma_{zz(hf)}(r,\theta,z) &= \int_0^\infty \xi J_0(\xi r)\left[g_5\partial^5 + h_5\partial^3 + l_5\partial\right]\left[A_{0(hf)}e^{-\lambda_1 z} + B_{0(hf)}e^{-\lambda_2 z} + C_{0(hf)}e^{-\lambda_3 z}\right]\mathrm{d}\xi
\end{aligned}
\tag{57}
$$

One may write the solutions for the case of all vertical and horizontal loads and the heat flux by adding the solutions given in Eqs. (47), (52) and (57), term by term. This case may define an arbitrary load applied on a circular patch. We can make differences among the radii of vertical load, horizontal load and heat flux, to have more complex case of external excitations.

5. Special problems

In the previous sections, the analytical results have been presented for general time-harmonic thermoelastic problem. In this section, two specific problems are considered to verify the formulations which are: (I) an elastodynamic problem without heat flux; and (II) an axisymmetric quasi-static thermoelastic problem.

Problem (I): *An elastodynamic problem without heat flux:*

It can be shown that if the thermal stress coefficient β is set to be zero, then the thermoelastodynamic problem can be degenerated to the elastodynamic one. If $\beta = 0$, then the operator in Eq. (20) is decomposed into two separate parts as

$$
\left(\partial^6 + I_{3e}(\xi)\,\partial^4 + I_{2e}(\xi)\,\partial^2 + I_{1e}(\xi)\right)\tilde{F}^m_m(\xi,z) = \left(\partial^4 + d_1\partial^2 + d_2\right)\left(\partial^2 + d_3\right)\tilde{F}^m_m(\xi,z) = 0 \tag{58}
$$

where in Eq. (58) and the later equations, the subscript e denotes the case of elastodynamics. In addition

$$
d_1 = \frac{-(3\mu+\lambda)}{(2\mu+\lambda)}\rho_0 p^2 - 2\xi^2,\; d_2 = \left(\rho_0 p^2 + \xi^2\right)\left(\frac{\mu\rho_0 p^2}{(2\mu+\lambda)} + \xi^2\right),\; d_3 = -\left(\xi^2 + \frac{pc}{k}\right) \tag{59}
$$

Denoting $\left(\partial^2 + d_3\right)\tilde{F}^m_m(\xi,z)$ by $\tilde{F}^m_{me}(\xi,z)$, one may eliminate the thermal effect and get the equation $\left(\partial^4 + d_1\partial^2 + d_2\right)\tilde{F}^m_{me}(\xi,z) = 0$, which considering the radiation conditions results in $\tilde{F}^m_{me}(\xi,z) = A_{me}(\xi)\,e^{-\lambda_{1e}z} + B_{me}(\xi)\,e^{-\lambda_{2e}z}$, where $\lambda^2_{ie}, (i=1,2)$ are the roots for the characteristic equation $\lambda^4_e + d_1\lambda^2_e + d_2 = 0$, whose solutions are $\lambda_{1e} = \bar{\alpha} = \sqrt{\xi^2 - k_d^2}$ and $\lambda_{2e} = \bar{\beta} = \sqrt{\xi^2 - k_s^2}$, with $k_d = \omega/C_\mathrm{d}, k_s = \omega/C_\mathrm{s}$, $C_\mathrm{d} = \sqrt{(2\mu+\lambda)/\rho}$ and $C_\mathrm{s} = \sqrt{\mu/\rho}$. Moreover, Eq. (21) remains unchanged in the case of elastodynamics, and its solution may be considered as $\tilde{\chi}^m_{me}(\xi,z) = C_{me}(\xi)\,e^{-\lambda_{3e}z}$, where one may readily show that $\lambda_{3e} = \lambda_{2e} = \bar{\beta}$. The displacements and stresses in the Fourier–Hankel transformed domain,$\tilde{u}^n_{ime}$ and $\tilde{\sigma}^n_{izme}; (i = r,\theta,z)$, are determined in terms of $\tilde{F}^m_{me}$ and $\tilde{\chi}^m_{me}$, respectively, based on Eqs. (32) and (33) when $\beta = 0$. For example, the stresses $\tilde{\sigma}^n_{izme}; (i = r,\theta,z)$ are written in terms of $\tilde{F}^m_{me}$ and $\tilde{\chi}^m_{me}$ as

$$\begin{aligned}\tilde{\sigma}^{m-1}_{rzme} - i\tilde{\sigma}^{m-1}_{\theta zme} &= -\left[g_4\partial^2 + h_{4e}\right]\tilde{F}^m_{me} + \left[g_6\partial\right]\tilde{\chi}^m_{me},\\ \tilde{\sigma}^{m+1}_{rzme} + i\tilde{\sigma}^{m+1}_{\theta zme} &= \left[g_4\partial^2 + h_{4e}\right]\tilde{F}^m_{me} + \left[g_6\partial\right]\tilde{\chi}^m_{me},\\ \tilde{\sigma}^m_{zzme} &= \left[g_5\partial^3 + h_{5e}\partial\right]\tilde{F}^m_{me}\end{aligned} \tag{60}$$

where

$$h_{4e} = \xi k\left[\frac{2\mu+\lambda}{\mu}\xi^2 - k_s^2\right], \quad h_{5e} = \frac{k}{\mu}\left[\left(2\mu+\lambda\right)k_s^2 - \left(4\mu+3\lambda\right)\xi^2\right] \tag{61}$$

Also it can be shown that if $\beta = 0$, according to Eq. (34), $g_{3e} = h_{3e} = 0$ and considering Eq. (32), the change of temperature that is coupled with the displacements is determined to be zero.

By virtue of Eq. (60) and the stress boundary conditions Eqs. $(31)_{a,b,c}$, one may obtain a 3×3 system of linear algebraic equations to be solved for A_{me}, B_{me} and C_{me}, whose solution is

$$\begin{aligned}A_{me} &= \left[y_{2e}\left(X_m - Y_m\right) + 2x_{2e}Z_m\right]/h_e\left(\xi\right),\\ B_{me} &= -\left[y_{1e}\left(X_m - Y_m\right) + 2x_{1e}Z_m\right]/h_e\left(\xi\right),\\ C_{me} &= \frac{X_m + Y_m}{2x_{3e}}, h_e\left(\xi\right) = 2\left(x_{2e}y_{1e} - x_{1e}y_{2e}\right)\end{aligned} \tag{62}$$

where

$$\begin{aligned}x_{ie} &= \left[g_4\lambda_{ie}^2 + h_{4e}\right], (i = 1,2), x_{3e} = -\left[g_6\right]\lambda_{3e},\\ y_{ie} &= -\left[g_5\lambda_{ie}^3 + h_{5e}\lambda_{ie}\right], (i = 1,2)\end{aligned} \tag{63}$$

Using Eq. (62), $\tilde{F}^m_{me}$ and $\tilde{\chi}^m_{me}$ are completely obtained, which may be used for determining the transformed displacements $\tilde{u}^n_{ime}\left(\xi, z\right)$ that via the use of the Hankel inverse theorem results in the displacements as

$$\begin{aligned}u_{rme}\left(r,z\right) &= \frac{1}{2}\int_0^\infty \xi\left\{\left[J_{m+1}\left(\xi r\right) - J_{m-1}\left(\xi r\right)\right]\left[g_1\partial\right]\left[A_{me}e^{-\lambda_{1e}z} + B_{me}e^{-\lambda_{2e}z}\right]\right.\\ &\quad \left. - i\xi\left[J_{m+1}\left(\xi r\right) + J_{m-1}\left(\xi r\right)\right]\left[C_{me}e^{-\lambda_{3e}z}\right]\right\}\mathrm{d}\xi,\\ u_{\theta me}\left(r,z\right) &= \frac{1}{2i}\int_0^\infty \xi\left\{\left[J_{m+1}\left(\xi r\right) + J_{m-1}\left(\xi r\right)\right]\left[g_1\partial\right]\left[A_{me}e^{-\lambda_{1e}z} + B_{me}e^{-\lambda_{2e}z}\right]\right.\\ &\quad \left. - i\xi\left[J_{m+1}\left(\xi r\right) - J_{m-1}\left(\xi r\right)\right]\left[C_{me}e^{-\lambda_{3e}z}\right]\right\}\mathrm{d}\xi,\\ u_{zme}\left(r,z\right) &= \int_0^\infty \xi J_{\mathrm{m}}\left(\xi r\right)\left[g_2\partial^2 - \frac{h_{4e}}{\xi\mu}\right]\left[A_{me}e^{-\lambda_{1e}z} + B_{me}e^{-\lambda_{2e}z}\right]\mathrm{d}\xi\end{aligned} \tag{64}$$

For a uniformly distributed vertical load of unit resultant applied on a circular disc of radius a acting in the z-direction, the Fourier series have only one term for $m = 0$, and thus one may simplified the displacements of Eq. (64) as follows

$$\begin{aligned}u_{re}\left(r,z\right) &= \frac{-1}{\pi\mu a}\int_0^\infty \gamma_3\left(z,\xi\right)J_1\left(\xi r\right)J_1\left(\xi a\right)\mathrm{d}\xi,\\ u_{\theta e}\left(r,z\right) &= 0,\\ u_{ze}\left(r,z\right) &= \frac{1}{\pi a\mu}\int_0^\infty \Omega_2\left(z,\xi\right)J_0\left(\xi r\right)J_1\left(\xi a\right)\mathrm{d}\xi,\end{aligned} \tag{65}$$

Similarly, for a uniformly distributed lateral load of unit resultant applied on a circular disc of radius a acting in the x-direction, the displacements of Eq. (64) are simplified as

$$u_{re}(r,\theta,z) = \frac{cos\theta}{2\pi\mu a}\left\{\int_0^\infty \gamma_1(z,\xi)\,J_1(\xi a)\left[J_0(\xi r) - J_2(\xi r)\right]\mathrm{d}\xi + \int_0^\infty \gamma_2(z,\xi)\,J_1(\xi a)\left[J_0(\xi r) + J_2(\xi r)\right]\mathrm{d}\xi\right\},$$

$$u_{\theta e}(r,\theta,z) = \frac{-sin\theta}{2\pi\mu a}\left\{\int_0^\infty \gamma_1(z,\xi)\,J_1(\xi a)\left[J_0(\xi r) + J_2(\xi r)\right]\mathrm{d}\xi + \int_0^\infty \gamma_2(z,\xi)\,J_1(\xi a)\left[J_0(\xi r) - J_2(\xi r)\right]\mathrm{d}\xi\right\},$$

$$u_{ze}(r,\theta,z) = \frac{cos\theta}{\pi\mu a}\int_0^\infty \Omega_1(z,\xi)\,J_1(\xi a)\,J_1(\xi r)\,\mathrm{d}\xi, \tag{66}$$

The displacements given in Eqs. (65) and (66) are exactly the same as the results presented in Pak [15] for surface excitation. $\gamma_1, \gamma_2, \gamma_3, \Omega_1$ and Ω_2 in Eqs. (65) and (66) are those intermediate parameters presented in Pak [15] for surface excitation (s=0). It should be noted that $\bar{\alpha}$ and $\bar{\beta}$ in this paper are, respectively, equivalent to α and β in the notation of Pak [15].

Problem (II): *An axisymmetric quasi-static thermoelastic problem*:

This is the case considered by Ding et al. [34]. It can be shown that in the case of axisymmetric problem, the potential function χ is omitted and the displacements and temperature are expressed in terms of only the scalar potential function F [43]. In this case, the Fourier expansion of any function has only one component, which is for $m = 0$. In addition, in the quasi-static problem, the density is set to be zero ($\rho = 0$). So considering axisymmetric as well as the quasi-static problem, one may find $\lambda_{1qs} = \lambda_{2qs} = \xi$ and $\lambda_{3qs} = \sqrt{\xi^2 + p/k_0}$, where $k_0 = k(2\mu+\lambda)/\left(c(2\mu+\lambda) + \beta^2 T_0\right)$ and the subscript qs denotes the quasi-static problem. Because of the existence of repeated roots $\lambda_{1qs} = \lambda_{2qs} = \xi$, the Eq. (24) for $m = 0$ is written as

$$\tilde{F}^0_{0qs}(\xi,z) = A_{0qs}(\xi)\,e^{-\xi z} + zB_{0qs}(\xi)\,e^{-\xi z} + C_{0qs}(\xi)\,e^{-\lambda_{3qs}z}. \tag{67}$$

By assuming the traction free surface, all the components of the external traction are set to zero, which results in $X_0 = Y_0 = Z_0 = 0$. Thus, the non-zero boundary condition is $\tilde{T}^0_{0qs}(\xi, z=0) = \tilde{H}^0_0(\xi) = W_0$. Satisfying both the homogeneous and non-homogeneous boundary conditions, as done in previous sections, the functions A_{0qs}, B_{0qs} and C_{0qs} are determined, and then same as the procedure we did before, the none-zero displacements and the temperature are obtained as the following improper line integrals

$$u_{rqs}(r,z) = \int_0^\infty \xi J_1(\xi r)\left[D_1 e^{-\xi z} + D_2 e^{-\lambda_{3qs}z} + (\lambda_{3qs} - \xi)\,D_2 z e^{-\xi z}\right]\mathrm{d}\xi,$$

$$u_{zqs}(r,z) = \int_0^\infty \xi J_0(\xi r)\left[D_3 e^{-\xi z} + \frac{\lambda_{3qs}}{\xi} D_2 e^{-\lambda_{3qs}z} + (\lambda_{3qs} - \xi)\,D_2 z e^{-\xi z}\right]\mathrm{d}\xi,$$

$$T_{qs}(r,z) = \int_0^\infty \xi J_0(\xi r)\left[D_4 e^{-\xi z} + D_5 e^{-\lambda_{3qs}z}\right]\mathrm{d}\xi \tag{68}$$

where

$$D_1 = \frac{\beta k\left(\left(\beta^2 T_0 + (2\mu+\lambda)\,c\right)\lambda_{3qs} - \mu c\xi\right)W_0}{\psi}, D_2 = \frac{-\beta k\xi\left(\beta^2 T_0 + (\mu+\lambda)\,c\right)W_0}{\psi},$$
$$D_3 = \frac{\beta k\left(\left(\beta^2 T_0 + (2\mu+\lambda)\,c\right)\xi - \mu c\lambda_{3qs}\right)W_0}{\psi}, D_4 = \frac{2\beta^2 T_0 k\xi\mu\left(\xi - \lambda_{3qs}\right)W_0}{\psi},$$
$$D_5 = \frac{p\left(\beta^2 T_0 + (\mu+\lambda)\,c\right)\left(\beta^2 T_0 + (2\mu+\lambda)\,c\right)W_0}{\psi},$$
$$\psi = \beta^4 T_0^2 p + \left(\lambda^2 + 3\lambda\mu + 2\mu^2\right)pc^2 + \beta^2 T_0\left((3\mu+2\lambda)\,pc + 2k\xi\mu\left(\xi - \lambda_{3qs}\right)\right). \tag{69}$$

Equation (68) should be the same as the results presented by Ding et al. [34]. However, there are some mistyping in Eq. (31) of Ding et al. [34], where the first two equations of Eq. (31) in their paper must be changed as follows

$$\begin{aligned} 2\rho c_1 + 2\rho c_2 + Bc_3 &= 0, \\ 2\rho c_1 + 2\left(\sqrt{\rho^2 + p/K_0}\right)c_2 + (B-2)\,c_3 &= 0 \end{aligned} \tag{70}$$

ξ, u_z, T and W_0 in this paper are, respectively, equivalent to ρ, w, θ and f^0 in the notation of Ding et al. [34].

6. Numerical integration and results discussion

As we have shown in the previous sections, the asymmetric responses of the thermoelastodynamic problem in an isotropic half-space such as displacement components, temperature difference and stress components have been presented in the forms of some semi-infinite line integrals due to applying arbitrary time-harmonic mechanical force field and heat flux. Because of complexities in the integrand functions due to existence of multi-valued functions (radical functions), exponential and Bessel functions, the integrals cannot be given in closed form and thus a numerical procedure is needed. The integrands also contain some branch points due to existence of multi-valued functions and pole, which needs some special attentions, when one implements a numerical procedure. As mentioned earlier, the thermoelastodynamic problem under consideration have four branch points $\xi_{\lambda_i}, (i = 1-4)$, where neither ξ_{λ_1} nor ξ_{λ_3} is located on the path of integration, but $\xi_{\lambda_2} = \xi_{\lambda_4}$ are pure real numbers and they are thus located on the path of integration. Also, the integrand functions have a singular point which is related to Rayleigh wave number. In the case of elastodynamics, $\xi_p = \sqrt{3+\sqrt{3}}\sqrt{\rho/\mu}\omega/2$ is the pole, which corresponds to the Rayleigh waves (see e. g., Pak [15]). In this paper, the Rayleigh pole can be calculated by solving the equation $h(\xi) = 0$. It is notable that due to thermomechanical coupling, the roots for equation $h(\xi) = 0$ are conjugate complex numbers in the complex ξ-plane. Therefore, the Rayleigh pole of integrand functions has an imaginary part, although it is small. Thus, the Rayleigh pole of the integrand functions dose not located on the path of integration, which is the positive real axis in the complex ξ-plane; however, the integrand is nearly singular on the real axis close to the above-mentioned pole. In the process of numerical integration, we should pay special attention to the branch points $\xi_{\lambda_2} = \xi_{\lambda_4}$ which are located on the path of integration. Moreover, the numerical evaluation of integrals needs careful consideration because of the oscillatory behavior of the integrands involving product of the Bessel functions. Because of the highly oscillatory nature of integrands, they tends to zero slowly when ξ approaches infinity. It makes the integrals to be converged too slowly. Considering the points mentioned here and for weakly singular behavior of the integrands near the Rayleigh pole ξ_p and branch points $\xi_{\lambda_2} = \xi_{\lambda_4}$, the "Global-Adaptive", "MaxErrorIncreases", "MaxRecursion", "MinRecursion" and "WorkingPrecision" features in the Mathematica Software are used for numerical evaluations of whole integrals involved in this paper.

Table 1. *Elastic coefficients and thermal properties of materials*

Material no.	$E\,(\mathrm{Nm}^{-2})$	υ	β
1	5×10^{10}	0.25	1
2	5×10^{10}	0.25	7.04×10^{6}
3	5×10^{10}	0.25	7.04×10^{8}

Table 2. *Numerical values of pole and branch points for* $\omega_0 = 0.5$

Material no.	ξ_{λ_1}	$\xi_{\lambda_2}=\xi_{\lambda_4}$	ξ_{λ_3}	ξ_p
$1\,(\beta=1)$	$\pm\,(0.2886+2.6078\times10^{-12}i)$	$\pm\,0.5$	$\pm\,(48.2451-48.2451i)$	$(0.5438-4.1926\times10^{-17}i)$
$2\,(\beta=7.04\times10^{6})$	$\pm\,(0.012-1.632\times10^{-8}i)$	$\pm\,0.5$	$\pm(1159.37-1159.37i)$	$(0.5234-2.3355\times10^{-9}i)$
$3\,(\beta=7.04\times10^{8})$	$\pm\,(0.00155+0.00155i)$	$\pm\,0.5$	$\pm(115836-115836i)$	$(0.5233-2.2932\times10^{-13}i)$

Table 3. *Numerical values of pole and branch points for* $\omega_0 = 3$

Material no.	ξ_{λ_1}	$\xi_{\lambda_2}=\xi_{\lambda_4}$	ξ_{λ_3}	ξ_p
$1\,(\beta=1)$	$\pm\,(1.732+1.738\times10^{-12}i)$	±3	$\pm\,(118.176-118.176i)$	$(3.2629-1.2157\times10^{-15}i)$
$2\,(\beta=7.04\times10^{6})$	$\pm\,(0.072+1.3056\times10^{-7}i)$	$\pm\,3$	$\pm(2839.86-2839.85i)$	$(3.1404-8.2397\times10^{-8}i)$
$3\,(\beta=7.04\times10^{8})$	$\pm\,(0.0079-0.0079i)$	$\pm\,3$	$\pm\,(283740-283740i)$	$(3.1403-8.2554\times10^{-12}i)$

To illustrate some results, several isotropic materials with different properties are considered as given in Table 1. All of these three thermoelastic materials have the same Poisson ratio ($\upsilon = 0.25$) and elastic modulus ($E = 5\times10^{10}\,(\mathrm{Nm}^{-2})$), while the thermal stress coefficients of these materials are different. Material 1, Material 2 and Material 3 are defined by $\beta = 1$, $\beta = 7.04\times10^{6}$ and $\beta = 7.04\times10^{8}\,(\mathrm{Nm}^{-2}\,\mathrm{deg}^{-1})$, respectively. The thermal properties of Cobalt in SI units which have been presented in Das et al. [55] as $k = 69\,\mathrm{Wm}^{-1}\,\mathrm{deg}^{-1}$, $\rho = 8836\,\mathrm{kgm}^{-3}$, $c = 427\,\mathrm{Jkg}^{-1}\,\mathrm{deg}^{-1}$ and $T_0 = 298^{\circ}\,K$ are used for all materials in this paper.

With the use of Mathematica software, the numerical values of pole and branch points for the selected materials are listed in Tables 2 and 3. To show the accuracy of the numerical evaluations, the radial displacement u_r for the case of elastodynamics, $\beta = 0$, is evaluated and compared with the solution presented in Pak [15]. Since β appears in the denominator of some fractions in the formulation of the problem, we cannot set it identically zero in the numerical evaluations. Therefore, for numerical evaluation in the case of elastodynamics, a sufficiently small value for β is required. Here, 10^{-10} has been selected. Figure 5 compares the normalized radial displacement $u_r(r=0,z)$ of this study with the results of Pak [15] for a dimensionless frequency $\omega_0 = a\omega\sqrt{\rho/\mu} = 0.5$ and $\lambda/\mu = 1$, due to a lateral load of unit resultant applied on a circular disc of radius a. The displacement is normalized as $4\pi\mu a u_r(r=0,z)/P$ where $P = 1$ is the magnitude of lateral load. It can be seen in the figure that the agreement between two results is excellent.

Table 4 compares the branch points and poles for thermoelastodynamic problem with those of elastodynamics. As we mentioned before and as it is clear from Eq. $(29)_b$, the branch points ξ_{λ_2} and ξ_{λ_4} are, respectively, corresponds to the shear wave numbers horizontally (SH) and vertically (SV) polarized, while the branch points ξ_{λ_1} and ξ_{λ_3} are corresponding to coupled compression (P) and thermal wave numbers (see [45]). This correspondence is remedy discovered by detailed investigations of Eqs. $(29)_{a,c}$ and Eqs. (30). Also, ξ_p is corresponding to the Rayleigh (Ray) wave number. As can be inferred from Table 4, contrary to elastodynamics, in thermoelastodynamics, the coupled dilatational and thermal; and the Rayleigh wave numbers are affected by thermomechanical coupling and undergoes some damping and dispersion. However, this damping for coupled dilatational and thermal wave number is significant but for Rayleigh wave number is negligible. Based on these points, the coupled dilatational and thermal; and

TABLE 4. *Comparison of branch points and poles for thermoelastodynamic and elastodynamic cases*

Problem type	$\omega_0 = 0.5$				$\omega_0 = 3$			
	ξ_{λ_1}	$\xi_{\lambda_2} = \xi_{\lambda_4}$	ξ_{λ_3}	ξ_p	ξ_{λ_1}	$\xi_{\lambda_2} = \xi_{\lambda_4}$	ξ_{λ_3}	ξ_p
Thermoelastodynamic material no. 2.	$\pm(0.012 - 1.632 \times 10^{-8}i)$	± 0.5	$\pm(1159.37 - 1159.37i)$	$(0.5234 - 2.3355 \times 10^{-9}i)$	$\pm(0.072 + 1.3056 \times 10^{-7}i)$	± 3.0	$\pm(2839.86 - 2839.85i)$	$(3.1404 - 8.2397 \times 10^{-8}i)$
Elastodynamic material no. 2.	$\beta = 0 \pm 0.28867$	± 0.5	–	0.543832	± 1.7320	± 3.0	-	3.26299

TABLE 5. *Numerical values of normalized temperature $T(r = 0, z = 0)$ with respect to different amounts of β under applying a uniform vertical dynamic load of resultant R on a circular disc of radius a with $\omega_0 = 0.5$*

β	$\beta = 10$	$\beta = 10^2$	$\beta = 10^3$	$\beta = 10^4$	$\beta = 2.5 \times 10^4$	$\beta = 5 \times 10^4$	$\beta = 10^5$
$\frac{\mu a^2 T}{RT_0}$	$0.0039 - 0.00025i$	$0.039 - 0.0025i$	$0.39 - 0.025i$	$3.903 - 0.251i$	$9.667 - 0.6191i$	$18.715 - 1.181i$	$33.175 - 1.992i$
β	$\beta = 2.5 \times 10^5$	$\beta = 5 \times 10^5$	$\beta = 10^6$	$\beta = 5 \times 10^6$	$\beta = 10^7$	$\beta = 5 \times 10^7$	$\beta = 10^8$
$\frac{\mu a^2 T}{RT_0}$	$46.203 - 2.329i$	$35.841 - 1.611i$	$20.815 - 0.916i$	$4.396 - 0.198i$	$2.202 - 0.1i$	$0.44 - 0.02i$	$0.22 - 0.01i$

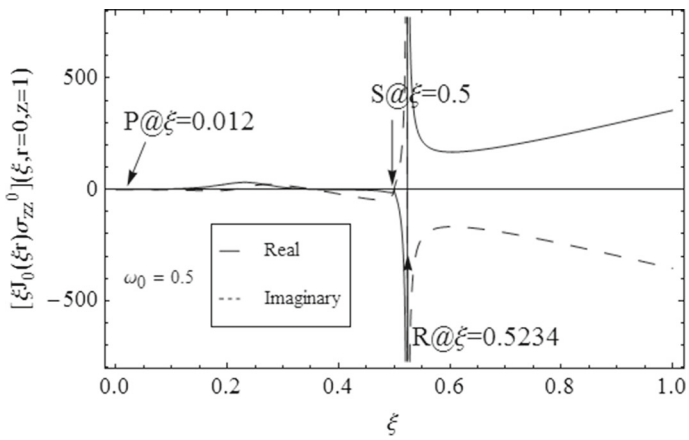

FIG. 3. Real and imaginary parts of integrand function of normal stress σ_{zz} subjected to unit temperature applied on a disc of radius a with $\omega_0 = 0.5$. The half-space is filled by material No. 2 (P = coupled dilatational and thermal wave; S = shear wave; and R = Rayleigh wave)

the Rayleigh wave speeds for thermoelastodynamic problem are larger than those of elastodynamics and these two waves arrive sooner in the thermoelastic material than elastic. Also it can be seen that both horizontal and vertical shear waves (SH and SV) are not affected by thermomechanical coupling and these two waves travel with the same velocities in the isotropic media.

Table 5 shows the numerical values of normalized temperature $T(r = 0, z = 0)$ with respect to different amounts of β under a uniform vertical dynamic load of resultant R on a circular disc of radius a with $\omega_0 = 0.5$. Also, Fig. 7 depicts the normalized temperature $\mu a^2 T/(RT_0)$ versus logarithm of $\beta(Log_{10}\beta)$ based on the information presented in Table 5.

Figures 3 and 4 depict the variation of the integrand function of normal stress σ_{zz} with respect to ξ subjected to a unit temperature ($\theta_0 = 1K^\circ$) distributed on a circular disc of radius a for frequencies $\omega_0 = 0.5$ and 3.0 and material No. 2. As can be seen from these figures, ξ_{λ_1} and ξ_{λ_3}, $\xi_{\lambda_2} = \xi_{\lambda_4}$ and ξ_p which are given in Tables 2 and 3 for thermoelastodynamic problem are, respectively, corresponds to coupled

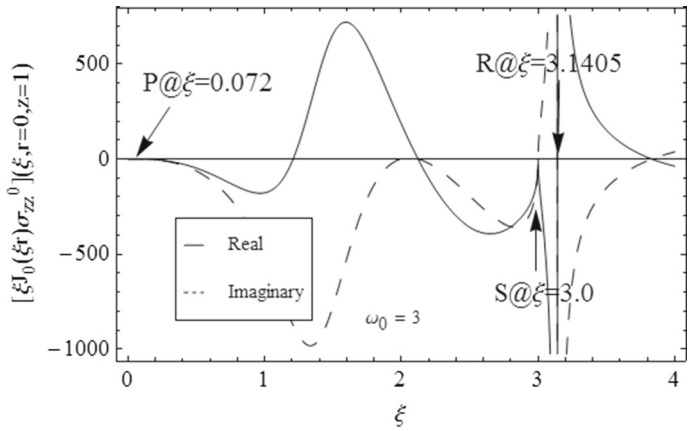

FIG. 4. Real and imaginary parts of integrand function of normal stress σ_{zz} subjected to unit temperature applied on a disc of radius a with $\omega_0 = 3$. The half-space is filled by material No. 2 (P = coupled dilatational and thermal wave; S = shear wave; and R = Rayleigh wave)

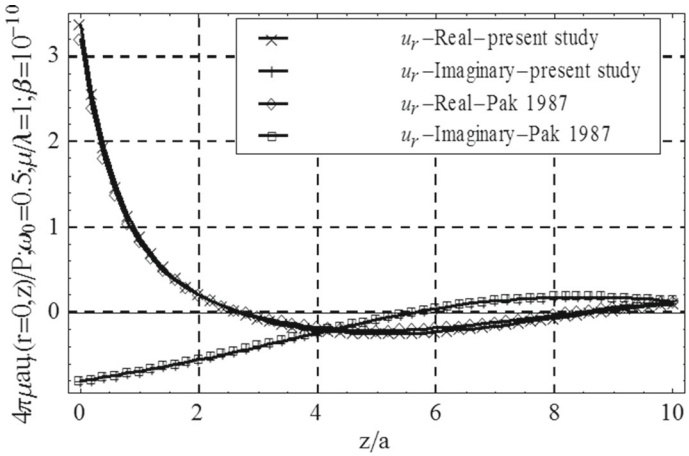

FIG. 5. Comparison of displacement in radial direction $u_r(r = 0, z)$ along z axis subjected to a uniform lateral load applied on a disc of radius a acting with frequency $\omega_0 = 0.5$ in elastic and thermoelastic half-spaces

dilatational and thermal (P), shear (S) and Rayleigh (Ray) wave numbers. Also, it can be inferred from these figures that the wave numbers are completely dependent on the frequency of excitation.

Three cases are defined to illustrate the numerical results. These cases are (1) a uniform vertical load of resultant $R = 1N$ applied on a circular patch of radius a, (2) a uniform horizontal load of resultant $P = 1N$ applied on a circular patch of radius a and (3) a uniform constant heat flux with intensity $H = q_0$ passing through a circular disc of radius a(see Fig. 1). The results are prepared in such a way to show the effect of different frequency of excitation and thermal properties of materials. To illustrate the numerical results graphically, some dimensionless parameters are defined. In the Case (1), we show the dimensionless displacement and stress as $\pi\mu a u_z/R$ and $\pi a^2\sigma_{zz}/R$, respectively, and the dimensionless temperature as $\mu a^2 T/(RT_0)$. In the case (2), $\pi\mu a u_r/P$ and $\mu a^2 T/(PT_0)$ are used as dimensionless displacement and temperature, respectively, and in the Case (3), $kT_0\sigma_{zz}/(a\mu q_0)$ is used as dimensionless stress. In the first two cases, R and P are the resultant forces. In addition, $\omega_0 = a\omega\sqrt{\rho/\mu}$ is used as the dimensionless

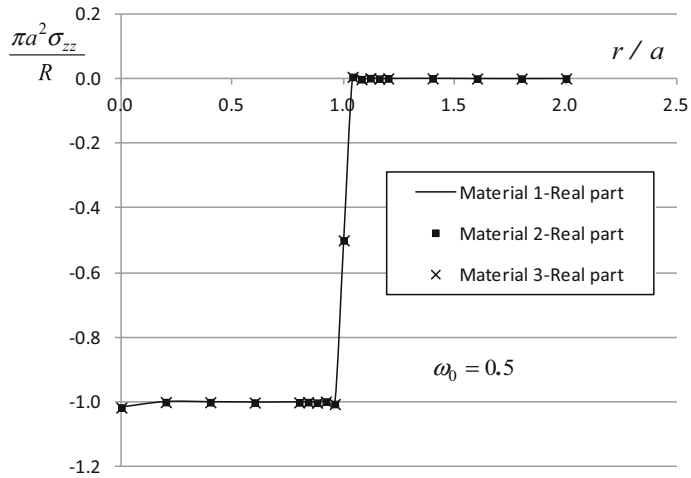

FIG. 6. Real part of normal stress σ_{zz} along r axis (i.e. $z = 0$) for materials number 1, 2 and 3 subjected to a uniform vertical dynamic load applied on a disc of radius a with $\omega_0 = 0.5$

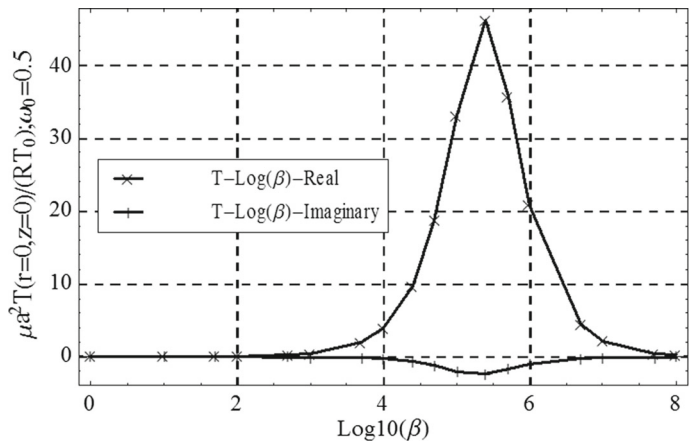

FIG. 7. Real and imaginary parts of normalized temperature $T(r = 0, z = 0)$ with respect to logarithm of β, under applying a uniform vertical dynamic load of resultant R on a circular disc of radius a with $\omega_0 = 0.5$

frequency. It is worthwhile to be mentioned that all dimensionless parameters for applying vertical and horizontal dynamic load and heat flux are defined such that these dimensionless functions be independent of thermal stress coefficient β. This selection makes it possible to track the direct effects of thermal-stress coefficient β on the responses; because all three materials defined in Table 1 have different thermal-stress coefficient β.

Figure 6 indicates that the normal stress (σ_{zz}) for $r \leq a$ is equal to the amount of traction applied on the surface of the medium, which shows the validity of the boundary conditions. Figure 7 depicted the real and imaginary parts of normalized temperature $\mu a^2 T/(RT_0)$ versus logarithm of $\beta(Log_{10}\beta)$ based on the information presented in Table 5. As can be seen from Fig. 7, by increasing β, the normalized temperature $\mu a^2 T/(RT_0)$ has been increased at first and then this function has been decreased until its amplitude tend to zero at very large amounts of β. This means that there is nonlinear relationship between the thermal-stress coefficient β and the displacement, temperature and stress responses. As can

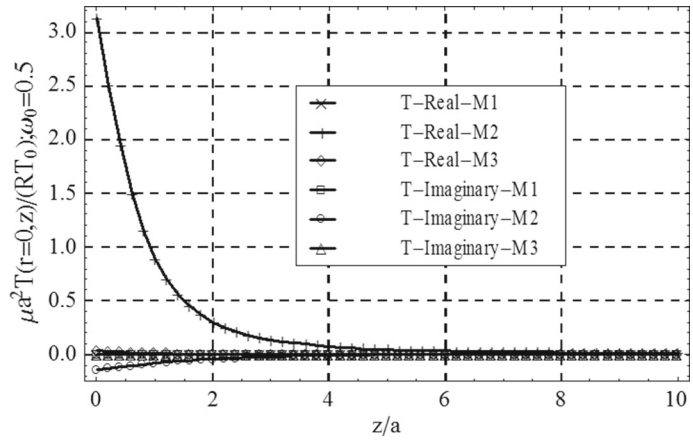

FIG. 8. Real and imaginary parts of normalized temperature $T(r = 0, z)$ subjected to a uniform vertical dynamic load applied on a disc of radius a with $\omega_0 = 0.5$

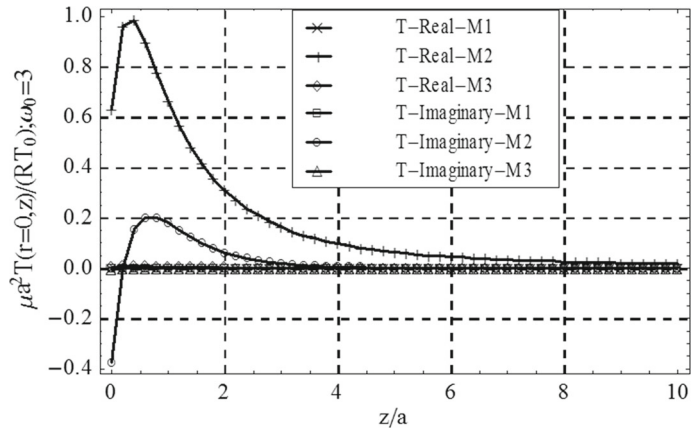

FIG. 9. Real and imaginary parts of normalized temperature $T(r = 0, z)$ subjected to a uniform vertical dynamic load applied on a disc of radius a with $\omega_0 = 3$

be seen from this figure, the curve of normalized temperature versus logarithm of β is very similar to the normal or Gaussian distribution (bell curve) in the probability theory.

Figures 8 and 9 illustrate the real and imaginary parts of normalized temperature $T(r = 0, z)$ subjected to uniform vertical dynamic load applied on a circular disc of radius a with $\omega_0 = 0.5$ and $\omega_0 = 3$ respectively. As can be seen from these two figures, the amplitudes of real and imaginary parts of normalized temperature for material number 2 in Table 1 are more than other two materials. The reason is that based on Table 5 and Fig. 7, for very small and very large amounts of thermal-stress coefficient β, the amplitude of normalized temperature is very small and therefore for material number 2 with $\beta = 7.04 \times 10^6$ the amplitude of normalized temperature is greater than other two materials.

In Figs. 10 and 11, the real and imaginary parts of normalized vertical displacement $\pi\mu a u_z(r = 0, z)/R$ subjected to uniform vertical dynamic load with resultant R applied on a circular disc of radius a with $\omega_0 = 0.5$ and $\omega_0 = 3$ are displayed, respectively. As can be seen in these figures, the higher the thermal stress coefficient (β), the lower the vertical displacement is, when the Poisson's ratio and other engineering

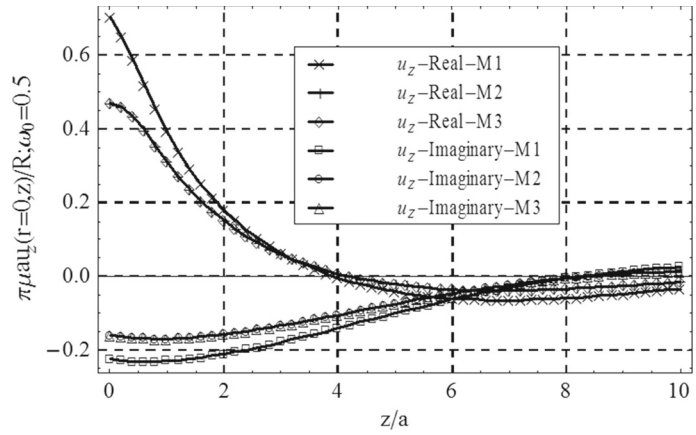

FIG. 10. Real and imaginary parts of normalized vertical displacement $u_z(r=0,z)$ subjected to a uniform vertical dynamic load with resultant R applied on a disc of radius a with $\omega_0 = 0.5$

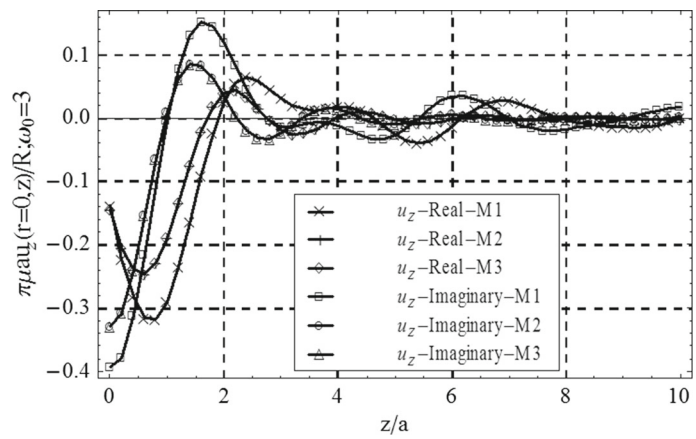

FIG. 11. Real and imaginary parts of normalized vertical displacement $u_z(r=0,z)$ subjected to uniform vertical dynamic load with resultant R applied on disc of radius a with $\omega_0 = 3$

properties are kept constants. This happens because of thermoelastic damping which is due to the effect of change of temperature in the thermoelastic media. This is the fact that Biot [18] also pointed out for the effect of damping on the change of temperature in the thermoelastic material. Because of the existence of damping, a small part of energy is dissipated and the response occurs due to the remaining energy. Moreover, it can be seen from these figures that the responses are absolutely affected by the frequency of excitation. As frequency increases, the responses have shown more oscillatory behavior.

Figure 12 depicted the real and imaginary parts of normalized temperature $\mu a^2 T(r=a,z)/(PT_0)$ subjected to uniform horizontal dynamic load with resultant P applied on a circular disc of radius a with $\omega_0 = 3$. As can be seen from this figure, also the amplitudes of real and imaginary parts of normalized temperature for material number 2 are more than other two materials.

Figure 13 depicted the real and imaginary parts of normalized radial displacement $\pi\mu a u_r(r=0,z)/P$ subjected to uniform horizontal dynamic load with resultant P applied on a circular disc of radius a with $\omega_0 = 0.5$. As can be seen from Fig. 13, the higher the thermal stress coefficient (β), the lower the radial displacement is, when the Poisson's ratio and other engineering properties are kept constants.

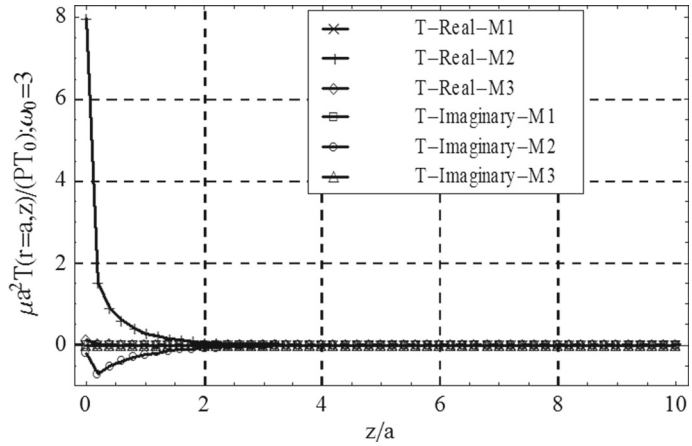

FIG. 12. Real and imaginary parts of normalized temperature T along z axis at $r = a$ subjected to a uniform horizontal dynamic load with resultant P applied on a disc of radius a with $\omega_0 = 3$

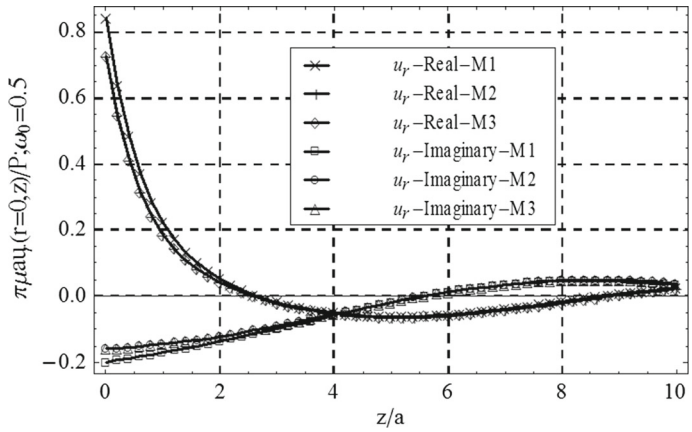

FIG. 13. Real and imaginary parts of normalized radial displacement $u_r(r = 0, z)$ subjected to uniform horizontal dynamic load with resultant P applied on disc of radius a with $\omega_0 = 0.5$

This happens because of thermoelastic damping which is due to the effect of change of temperature in the thermoelastic media. Figures 14, 15 and 16 illustrated the real and imaginary parts of normalized normal stress $kT_0\sigma_{zz}/(a\mu q_0)$ in a different radial or depth for frequencies $\omega_0 = 0.5$ and $\omega_0 = 3$ subjected to a constant heat flux q_0 passing through a circular disc of radius a. As can be seen, the amplitudes of real and imaginary parts of normalized normal stress for material number 2 are more than other two materials. This behavior is similar to behavior of normalized temperature under applying uniform vertical and horizontal dynamic load (Figs. 8, 9 and 12).

Figures 17 and 18, respectively depicted the real and imaginary parts of normalized vertical displacement and normal stress functions subjected to a uniform vertical dynamic load applied on a disc of radius a, versus the dimensionless frequency ω_0. Figure 17 shows that by increasing the dimensionless frequency ω_0, the amplitudes of both real and imaginary parts of normalized displacement have been decreased, while Fig. 18 shows that by increasing ω_0, the amplitudes of both real and imaginary parts of normalized

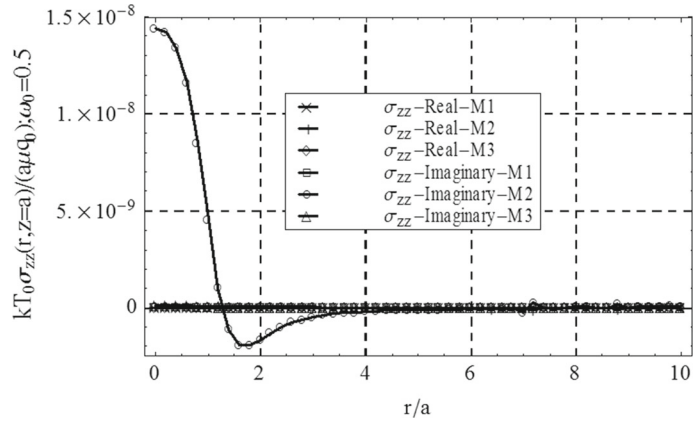

FIG. 14. Real and imaginary parts of normalized normal stress $\sigma_{zz}(r, z = a)$ subjected to a constant heat flux q_0 passing through a circular disc of radius a with $\omega_0 = 0.5$

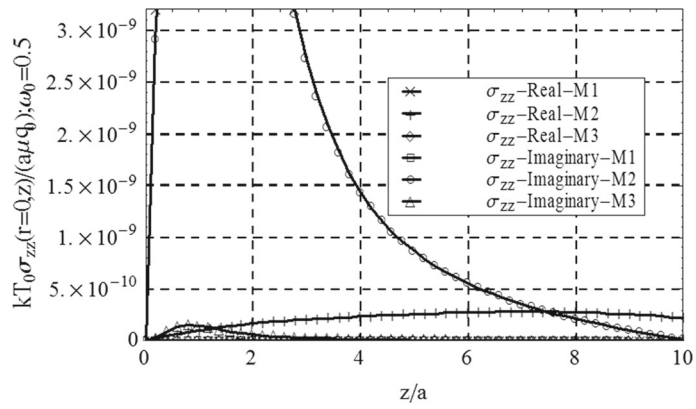

FIG. 15. Real and imaginary parts of normalized normal stress $\sigma_{zz}(r = 0, z)$ subjected to a constant heat flux q_0 passing through a circular disc of radius a with $\omega_0 = 0.5$

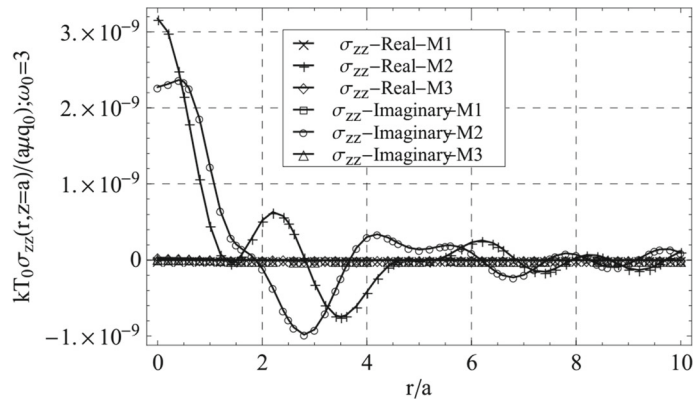

FIG. 16. Real and imaginary parts of normalized normal stress $\sigma_{zz}(r, z = a)$ of a half-space subjected to a constant heat flux q_0 passing through a circular disc of radius a with $\omega_0 = 3$

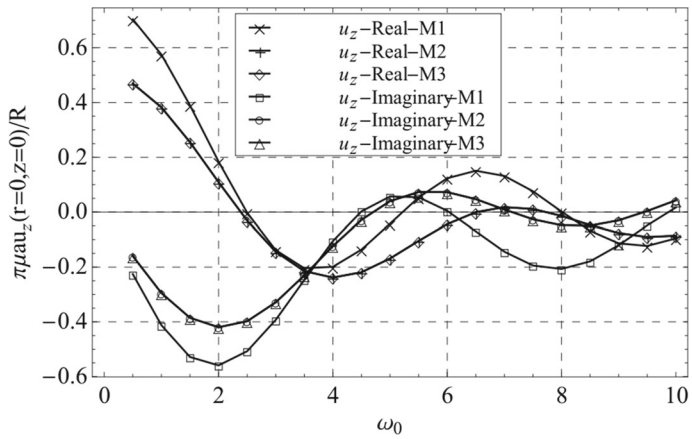

FIG. 17. Real and imaginary parts of normalized vertical displacement $u_z(r = 0, z = 0)$ of a half-space subjected to a uniform vertical dynamic load with resultant R applied on a disc of radius a; versus the dimensionless frequency ω_0

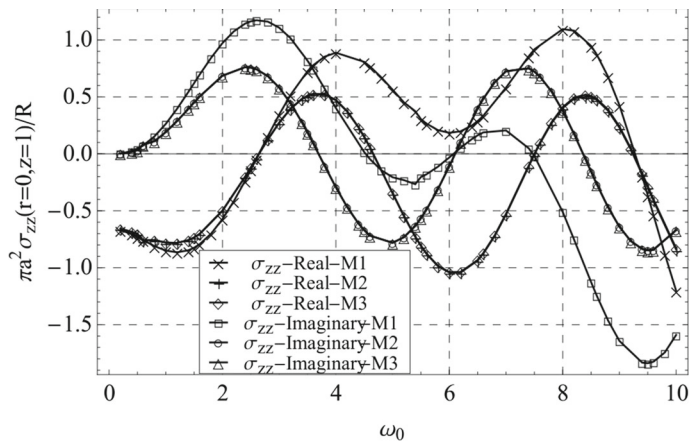

FIG. 18. Real and imaginary parts of normalized normal stress $\sigma_{zz}(r = 0, z = 1)$ of a half-space subjected to a uniform vertical dynamic load with resultant R applied on a disc of radius a; versus the dimensionless frequency ω_0

normal stress are increased slightly. In addition, based on these two figures, by increasing the dimensionless frequency ω_0, both displacement and stress functions have shown more oscillatory behavior at a special point within the domain.

7. Conclusion

A half-space containing linear thermoelastic material has been analytically investigated for the displacements, stresses and temperature induced by arbitrary surface traction and heat flux boundary conditions. Two scalar potential functions have been utilized for uncoupling the set of equations of motion and energy equation within Biot's coupled thermoelasticity. The governing partial differential equations for the potential functions have been solved using the Fourier expansion and Hankel integral transforms in a cylindrical coordinate system. The unknown functions in the solutions for the potential functions have been numerically evaluated by satisfying the boundary conditions for three specific cases of vertical and

horizontal time-harmonic circular patch traction and a constant heat flux on the same circular patch. Based on the numerical results for change of temperature and normal stress, we conclude that there is nonlinear relationship between the thermal-stress coefficient β and the amplitude of temperature and stress responses. The solution may be used as the kernels in the integral methods such as boundary integral equations. Some points are mentioned about wave propagation in thermoelastodynamics and compared with elastodynamics. It is shown that, although the dilatational and Rayleigh wave speeds in thermoelastodynamic case are more than elastodynamics, the shear wave speeds in both cases are the same.

Acknowledgements

The partial support from University of Tehran through 27840/1/08 to M. E. -G. during this work is gratefully acknowledged.

References

[1] Barone, S., Patterson, E.A.: Polymer coating as a strain witness in thermoelasticity. J. Strain Anal. Eng. Des. **33**(3), 223–232 (1998)
[2] Mackin, T., Purcell, T.: The use of thermoelasticity to evaluate stress redistribution and notch sensitivity in ceramic matrix composites. Exp. Tech. **20**(2), 15–20 (1996)
[3] Varli, E.: Analysis of stress in a solid cylinder with periodic heat generation. A thesis submitted to the graduate school of natural and applied sciences-Middle East Technical University (2015)
[4] Sakagami, T., Izumi, Y., Kubo, S.: Successful application of thermoelasticity to remote inspection of fatigue cracks. In: Thermomechanics and Infra-Red Imaging, vol. 7, pp. 99-106. Springer (2011)
[5] Bills, B.G.: Thermoelastic bending of the lithosphere: implications for basin subsidence. Geophys. J. Int. **75**(1), 169–200 (1983)
[6] Sclater, J.G., Francheteau, J.: The implications of terrestrial heat flow observations on current tectonic and geochemical models of the crust and upper mantle of the earth. Geophys. J. Int. **20**(5), 509–542 (1970)
[7] Parker, R., Oldenburg, D.: Thermal model of ocean ridges. Nature **242**(122), 137–139 (1973)
[8] Davis, E., Lister, C.: Fundamentals of ridge crest topography. Earth Planet. Sci. Lett. **21**(4), 405–413 (1974)
[9] Lanzano, P.: Thermoelastic deformations of the Earth's lithosphere: a mathematical model. Earth Moon Planet. **34**(3), 283–304 (1986)
[10] Lamb, H.: On the propagation of tremors over the surface of an elastic solid. Philos. Trans. R. Soc. Lond. Ser. A Contain. Pap. Math. Phys. Character **203**, 1–42 (1904)
[11] Love, A.E.H.: A Treatise on the Mathematical Theory of Elasticity. Dover Publications, New York (1944)
[12] Ewing, W.M., Jardetzky, W.S., Press, F.: Elastic Waves in Layered Media. McGraw-Hill, Bengaluru (1957)
[13] Achenbach, J.D.: Wave Propagation in Elastic Solids. North-Holland Publishing Company, Amesterdam (1975)
[14] Aki, K., Richards, P.G.: Quantitative Seismology: Theory and Methods, vol. 1. W. H. Freeman and Co., New York (1980)
[15] Pak, R.Y.S.: Asymmetric wave propagation in an elastic half-space by a method of potentials. J. Appl. Mech. **54**(1), 121–126 (1987)
[16] Nowinski, J.L.: Theory of Thermoelasticity with Applications, vol. 3. Sijthoff and Noordhoff International Publishers, Alphen aan den Rijn (1978)
[17] Carlson, D.E.: Linear Thermoelasticity, Mechanics of Solids, vol. 2. Springer, Berlin (1972)
[18] Biot, M.A.: Thermoelasticity and irreversible thermodynamics. J. Appl. Phys. **27**(3), 240–253 (1956)
[19] Lessen, M.: Thermoelasticity and thermal shock. J. Mech. Phys. Solids **5**(1), 57–61 (1957)
[20] Deresiewicz, H. : Solution of the equations of thermoelasticity. In: Proceedings of the third U.S. National Congress of Applied Mechanics (1958)
[21] Zorski, H.: Singular solutions for thermoelastic media. Bull. Acad. Pol. Sci. **6**, 331–339 (1958)
[22] Novatskii, V.: Problems of thermoelasticity. Izd. Akad. Nauk SSSR, Moscow, 364 (1962)
[23] Nowacki, W.: Thermoelasticity. International Series of Monographs on Aeronautics and Astronautics, vol. 3. Solid and Structural Mechanics. Reading, Addison-Wesley Pub. Co., Division I (1962)
[24] Nowacki, W.: Green functions for the thermoelastic medium. Bull. Acad. Pol. Sci. Ser. Sci. Tech. **12**(9), 465–472 (1964)

[25] Nowacki, W.: On the completeness of stress functions in thermoelasticity. Bull. Acad. Pol. Sci. Ser. Sci. Tech. **15**(9), 583–591 (1967)
[26] Nowacki, W.: Dynamic Problems of Thermoelasticity. Springer, Dordrecht (1975)
[27] Verruijt, A.: The completeness of Biot's solution of the coupled thermoelastic problem. Q. Appl. Math. **26**, 485–490 (1969)
[28] Chandrasekharaiah, D., Srikantiah, K.: Waves of general type propagating in a liquid layer sandwiched between two thermo-elastic half-spaces. Int. J. Eng. Sci. **22**(3), 301–310 (1984)
[29] Chandrasekharaiah, D., Srikantiah, K.: Edge waves in a thermoelastic plate. Int. J. Eng. Sci. **23**(1), 65–77 (1985)
[30] Chandrasekharaiah, D.: Heat-flux dependent micropolar thermoelasticity. Int. J. Eng. Sci. **24**(8), 1389–1395 (1986)
[31] Chandrasekharaiah, D.: Thermoelasticity with second sound: a review. Appl. Mech. Rev. **39**(3), 355 (1986)
[32] Chandrasekharaiah, D.: One-dimensional wave propagation in the linear theory of thermoelasticity without energy dissipation. J. Therm. Stresses **19**(8), 695–710 (1996)
[33] Georgiadis, H., Rigatos, A., Brock, L.: Thermoelastodynamic disturbances in a half-space under the action of a buried thermal/mechanical line source. Int. J. Solids Struct. **36**(24), 3639–3660 (1999)
[34] Ding, H., Guo, F., Hou, P.: General solutions of coupled thermoelastic problem. Appl. Math. Mech. **21**(6), 631–636 (2000)
[35] Lykotrafitis, G., Georgiadis, H., Brock, L.: Three-dimensional thermoelastic wave motions in a half-space under the action of a buried source. Int. J. Solids Struct. **38**(28), 4857–4878 (2001)
[36] Sharma, J.: On the propagation of thermoelastic waves in homogeneous isotropic plates. Indian J. Pure Appl. Math. **32**(9), 1329–1342 (2001)
[37] Svanadze, M.: Fundamental solutions of the equations of the theory of thermoelasticity with microtemperatures. J. Therm. Stresses **27**(2), 151–170 (2004)
[38] Babaei, M., Abbasi, M., Eslami, M.: Coupled thermoelasticity of functionally graded beams. J. Therm. Stresses **31**(8), 680–697 (2008)
[39] Scalia, A., Svanadze, M.: Potential method in the linear theory of thermoelasticity with microtemperatures. J. Therm. Stresses **32**(10), 1024–1042 (2009)
[40] Sheng, G., Wang, X.: Thermoelastic vibration and buckling analysis of functionally graded piezoelectric cylindrical shells. Appl. Math. Model. **34**(9), 2630–2643 (2010)
[41] Scalia, A., Svanadze, M., Tracinà, R.: Basic theorems in the equilibrium theory of thermoelasticity with microtemperatures. J. Therm. Stresses **33**(8), 721–753 (2010)
[42] Kumar, R., Panchal, M.: A study of axi-symmetric waves through an isotropic thermoelastic diffusive medium. Comput. Appl. Math. **30**(2), 247–265 (2011)
[43] Eskandari-Ghadi, M., Sture, S., Rahimian, M., Forati, M.: Thermoelastodynamics with scalar potential functions. J. Eng. Mech. **140**(1), 74–81 (2013)
[44] Eskandari-Ghadi, M., Rahimian, M., Sture, S., Forati, M.: Thermoelastodynamics in transversely isotropic media with scalar potential functions. J. Appl. Mech. **81**(2), 021013 (2014)
[45] Raoofian-Naeeni, M., Eskandari-Ghadi, M., Ardalan, A.A., Pak, R.Y.S., Rahimian, M., Hayati, Y.: Coupled thermo-viscoelastodynamic Green's functions for bi-material half-space. ZAMM **95**(3), 260–282 (2013)
[46] Youssef, H.M., El-Bary, A.A.: Thermoelastic material response due to laser pulse heating in context of four theorems of thermoelasticity. J. Therm. Stresses **37**(12), 1379–1389 (2014)
[47] Hayati, Y., Eskandari-Ghadi, M., Raoofian, M., Rahimian, M., Ardalan, A.A.: Dynamic Green's functions of an axisymmetric thermoelastic half-space by a method of potentials. J. Eng. Mech. **139**(9), 1166–1177 (2012)
[48] Hayati, Y., Eskandari-Ghadi, M., Raoofian, M., Rahimian, M., Ardalan, A.A.: Frequency domain analysis of an axisymmetric thermoelastic transversely isotropic half-space. J. Eng. Mech. **139**(10), 1407–1418 (2012)
[49] Hetnarski, R.B., Eslami, M.R.: Thermal Stresses—Advanced Theory and Applications. Springer, Dordrecht (2008)
[50] Truesdell, C., Antman, S.S., Carlson, D.E., Fichera, G., Gurtin, M.E., Naghdi, P.M.: Mechanics of Solids. : Volume II: Linear Theories of Elasticity and Thermoelasticity, Linear and Nonlinear Theories of Rods, Plates, and Shells. Springer, Berlin (1984)
[51] Eringen, A.C., Şuhubi, E.S.: Elastodynamics: Linear theory, vol. 2. Academic Press, The University of Michigan, Ann Arbor (1975)
[52] Sneddon, I.N.: The Use of Integral Transforms. McGraw-Hill, New York (1972)
[53] Ablowitz, M.J., Fokas, A.S.: Complex Variables: Introduction and Applications. Cambridge University Press, Cambridge (2003)
[54] Rahimian, M., Eskandari-Ghadi, M., Pak, R.Y.S., Khojasteh, A.: Elastodynamic potential method for transversely isotropic solid. J. Eng. Mech. **133**(10), 1134–1145 (2007)
[55] Das, N., Lahiri, A., Sarkar, S.: Eigenvalue approach to three dimensional coupled thermoelasticity in a rotating transversely isotropic medium. Tamsui Oxford J. Math. Sci **25**(3), 237–257 (2009)

Yazdan Hayati
Department of Civil and Environmental Engineering
Amirkabir University of Technology
Tehran
Iran
e-mail: yhayati@aut.ac.ir

Morteza Eskandari-Ghadi
School of Civil Engineering, College of Engineering
University of Tehran
P. O. Box 11165-4563
Tehran
Iran
e-mail: ghadi@ut.ac.ir

(Received: July 19, 2017; revised: January 3, 2018)